JOURNAL OF GEOPHYSICAL RESEARCH, VOL. 102, NO. D6, PAGES 6883–6910, MARCH 27, 1997

Surface solar irradiance from the International Satellite Cloud Climatology Project 1983-1991

James K. B. Bishop,[1,2] William B. Rossow[1] and Ellsworth G. Dutton[3]

Abstract. An 8 year (July 1983 through June 1991) time series of daily and monthly mean surface solar irradiance has been produced for the globe using data from the International Satellite Cloud Climatology Project (ISCCP) and a revised Bishop and Rossow [1991] algorithm. We present a detailed validation analysis of the ISCCP solar irradiance fields with contemporaneous surface observations at buoys, at remote islands, and from the Global Energy Balance Archives (GEBA) [Ohmura et al., 1991]. The validation is hampered to some degree by the scale difference between the 280 km ISCCP product and the single-point measurements, some of which are affected by orographic clouds and other local meteorological effects. Our analysis suggests criteria for siting of island or coastal monitoring locations to minimize such biases. Particularly, eastward or poleward facing oceanic exposures are to be avoided. In addition, we suggest that deep sea buoys should be investigated for validation of oceanic surface fluxes. At open-ocean, clean-air sites, the ISCCP product is shown to be good to within 10 W m^{-2} in the monthly mean. The high-frequency (daily) systematics of solar irradiance variability at the open-ocean sites are also well duplicated by the ISCCP product. An identifiable error in the revised solar irradiance product is the neglect of spatially and temporally varying aerosol extinction. This error, when translated into an equivalent aerosol extinction coefficient, can be as large as 0.6 in known polluted and mineral dust-affected regions. We cannot determine additional satellite sensor calibration errors beyond those already corrected in the ISCCP processing. This uniquely long data set has been publicly available since 1994 at the National Center for Atmospheric Research. The data documents significant differences in solar fluxes received by the major oceans as well as significant flux variability on seasonal to interannual timescales.

1. Introduction

Surface solar irradiance is a key parameter determining global photosynthesis rates and the global energy balance. Its variability on small (<100 km) space scales and fast (hours) time scales is intimately tied to the variability of weather systems. Its observation from remote sensing platforms provides high spatial and temporal resolution so that its variability can be characterized.

Bishop and Rossow (BR) [1991] computed daily solar irradiance fields for the globe using cloud optical properties derived from the International Satellite Cloud Climatology Project (ISCCP), whose primary data sources are the four geostationary and two polar orbiting weather satellites [*Rossow and Schiffer*, 1991]. Other satellite surface solar irradiance data sets that span up to 4.5 years are those based on data from the Earth Radiation Budget Experiment (ERBE) [*Li and Leighton*, 1993; *Li*, 1995] and the Surface Radiation Budget (SRB) project [*Pinker et al.*, 1995]. The focus of these efforts has been to produce monthly mean fields for energy balance studies.

We have recomputed solar irradiance fields for the globe for July 1983 to June 1991 at monthly and daily temporal resolution and 280 km spatial resolution using a modified *Bishop and Rossow* [1991] algorithm. This 8 year time series, herein referred to as BR2, is also derived from ISCCP data. The central motivation for our effort differs from most other efforts in that we aim to produce surface solar irradiance and photosynthetically active irradiance (PAR) fields on timescales as short as 3 hours and spatial scales of 280 km and 30 km to support analysis of ocean productivity using phytoplankton chlorophyll biomass fields derived from the sea-viewing wide field-of-view sensor (SeaWiFS) ocean color radiometer [*Hooker and Esaias*, 1993]. The requirement for daily or shorter temporal resolution is dictated by the fact that oceanic phytoplankton can double their abundance as fast as once per day. Furthermore, plant distribution in the euphotic zone, and hence their light environment, is dictated by mixing which in turn is controlled in part by short-term variability in the air-sea heat budget in which solar irradiance is a dominant component (see, for example, *Stramska et al.* [1995]; *Bishop et al.* [1992]). Biological applications of the BR and BR2 data include efforts by *Mitchell et al.* [1991], *Potter et al.* [1993], and *Kahru et al.* [1994] to model productivity of the southern oceans and of global terrestrial ecosystems and to investigate causes of increased cyanobacteria blooms in the Baltic Sea, respectively.

Recent physical applications of the BR and BR2 (described by this paper) data sets include those of *Liu et al.* [1994] and *Seager and Blumenthal* [1994] in studies of the global ocean heat balance and of the heat balance of the tropical Pacific Ocean, respectively. *Seager and Blumenthal* [1994], in particular, found that including BR2 surface fluxes in their model of the tropical Pacific, as opposed to traditional bulk formula values (which depend only on cloud fraction and solar geometry), greatly improved the performance of their models. They further compared the BR2 data to those from ERBE [*Li et al.*, 1993] and found differences in surface solar irradiance of the order of 10 W m^{-2} (BR2 higher) on an annual

[1]NASA Goddard Institute for Space Studies, Goddard Space Flight Center, New York.

[2]Also at School of Earth and Ocean Sciences, University of Victoria, British Columbia, Canada.

[3]NOAA Climate Monitoring and Diagnostics Laboratory, Boulder, Colorado.

Paper number 96JD03865.
0148-0227/97/96JD03865 $09.00

mean basis for the oceans. A correspondence between the occurrence of high clouds and the difference (BR2-ERBE) was noted. Intercomparison of satellite data products does not validate one over another, however, either satellite data set improved model simulation of sea surface temperature in the tropics.

Cess et al [1995], using ERBE data and surface observations, suggested that clouds are more strongly absorbing of short wave solar irradiance than previously thought. They concluded that there may be a globally averaged +25 W m^{-2} error in surface short wave irradiance from satellite retrievals. The questions raised by their work require further data analysis.

This paper describes modifications made to the *Bishop and Rossow* (BR) algorithm (section 2) and validation efforts using a much expanded set of surface observations (section 3). Details pertaining to the satellite data processing are in the Appendix. We extend our analysis of the data to investigate surface solar irradiance variability on daily to interannual timescales with particular emphasis on the oceans (section 4). We will demonstrate that temporal and spatial variability described below is significantly in excess of any error associated with the data sets.

2. ISCCP Data and Surface Solar Irradiance Algorithm

The modified *Bishop and Rossow* [1991] scheme uses 280 km spatial resolution data from the International Satellite Cloud Climatology Project Briefly, ISCCP, beginning in July 1983, combines data from multiple geostationary and polar orbiting meteorological satellites to provide a global view of the occurrence and optical properties of clouds [*Schiffer and Rossow*, 1983, 1985, *Rossow et al*, 1985, and *Rossow and Schiffer*, 1991]. The current ISCCP data production spans July 1983 - June 1991 but will extend at least through 2000, thus providing overlap with SeaWiFS.

2.1 ISCCP C1/D1 and CX/DX Data

This paper describes the product of ISCCP C1 data which contains, at nominal 280 km resolution and every 3 hours for the globe, information about clouds, the atmosphere, and surface [*Rossow et al*, 1991; *Rossow and Schiffer*, 1991] For simplicity we have converted the ISCCP equal area data grid into a regular 2.5° by 2.5° grid in latitude and longitude

The ISCCP CX data is the high-resolution (4 7 km pixel size, regularly sampled at 30 km spatial intervals) data set used to generate C1 data (Figure 1). We mention the high-resolution data because it is important to emphasize the composite nature of the 280 km C1 data and that the C1 average quantities do not capture the spatial variability within the C1 pixel. The latter is important in the comparison with validation data sets (section 3). Also, 30 km data will be used to produce higher spatial resolution surface solar irradiance fields as the next step in our SeaWiFS efforts.

Specific C1 parameters used in our scheme are (1) solar zenith angle, (2) atmospheric ozone column abundance, total precipitable water, and surface pressure (daily for each 2 5° region, from TIROS operational vertical sounder (TOVS) data), (3) surface visible (at 600 nm) reflectance (every 3 hours for each 2.5° region), and (4) cloud parameters for a single layer: cover fraction, and optical thickness (at 600 nm) (every 3 hours for each 2.5° region). A limitation is that retrievals of cloud optical thickness are performed only when the solar zenith angle is less than 78.5°. A solution to this problem is outlined in the Appendix. Additional data sets employed are: (5) land-water fraction and (6) snow and sea ice cover (every 5 days for each 1 region) Although the ISCCP data

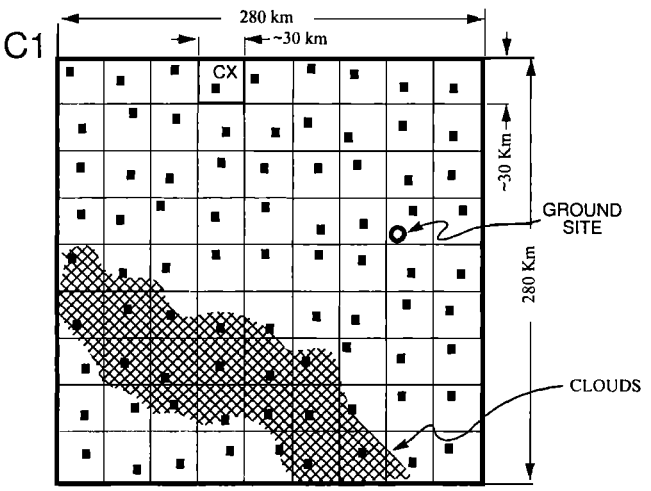

Figure 1. Schematic of International Satellite Cloud Climatology Project (ISCCP) CX and C1 pixels during one 3-hour time slice sampled by ISCCP. Also shown are the relationship of ground observation and cloud occurrence within the 280 km C1 pixel. C1 pixels represent the average values of cloud properties in approximately 80 30 km sized CX pixels. The CX pixel represents data randomly subsampled from a single 4-7 km area within that region.

are available eight times per day for most of the globe, regions not covered by geostationary satellite are observed less frequently by polar orbiters, leading to occasional gaps in the data.

The revisions to the Bishop and Rossow scheme and input data sets (and the resulting 8 year time series data produced) include (1) Satellite radiance calibration adjustments whereby C1 radiance data for the NOAA 7 period (July 1983 to January 1985) were multiplied by 0.945, those for the NOAA 9 period (February 1985 to October 1988) were unaltered, and those for the NOAA 11 period (November 1988 to June 1991) were multiplied by 1.119; (2) a scheme to trap and replace unexpected bad data; (3) an improved scheme to fill missing data; and (4) other modifications to the BR scheme. These are described in the Appendix.These steps were necessary to implement production of global surface solar irradiance fields on 3 hour time steps as required by SeaWiFS. The Appendix also describes the availability of data and an analysis of the effects of the revisions on published data produced with the original BR scheme.

ISCCP has begun to produce revised data sets named D1 and DX which will replace the "C" versions used for the BR2 data. The revisions made to the "D" series address some of the problems identified in revisons 1 and 2 above. We later use surface solar irradiance fields produced from DX data for March 1991 to illustrate differences between the surface observations and satellite retrievals at different spatial resolutions.

3. Validation of BR2 Surface Solar Irradiance Data

Validation of BR results was limited, particularly over the oceans Calculated monthly mean irradiances for July 1983 to July 1984 were compared with climatology from the 1970s at temperate latitude ocean weather stations. The comparison showed agreement within published estimates of interannual variability of monthly means at the individual stations. A further test was provided by the First ISCCP Regional Experiment/ Surface Radiation Budget FIRE/SRB experiment [*Whitlock et al.* 1990] wherein a 17 day timeseries October to November 1986 was obtained at a conti-

nental site in Wisconsin (43°N, 90°W) with a wide range (13 – 170 W m^{-2}) of daily averaged irradiance. In this case, excellent agreement was found.

Here we present new validation analyses of the BR2 solar irradiance fields. We will revisit the FIRE/SRB comparison (section 3.1). We have also compared our daily all-sky (including the effects of clouds) and clear sky data, to daily averages derived from contemporaneous high-frequency (<20 min) data sets obtained from sensors deployed on ocean moorings during the 1987 BioWATT [*Dickey et al.*, 1993] and the 1989 and 1991 Marine Light Mixed Layer (MLML) (*Dickey et al.* [1994], *Pluddeman et al.* [1995]) experiments (section 3.2). A further validation effort employs hourly resolved data sets obtained from island locations of Samoa, Kwajalein, Cape Grim, and Bermuda. The Samoa and Cape Grim data sets are the best long-term records available for comparison with the 8 year time series and were used in the *Cess et al.* [1995] analysis (sections 3.3 and 3.4). The comparison of a 0.5° DX-based surface irradiance field was used to investigate the representativeness of ocean island locations for validating surface irradiance over the ocean (section 3.5). Additionally, we have undertaken an analysis of the contemporaneous and extensive monthly irradiance observations available for oceanic island, land and coastal locations from the Global Energy Balance Archives (GEBA) [*Ohmura et al.*, 1991] (sections 3.6 and 3.7). A final comparison of our 8 year climatology is made with the historical monthly mean observations from the same five temperate latitude ocean weather stations investigated by BR (section 3.8).

3.1. FIRE/SRB Wisconsin Comparison

The *Bishop and Rossow* [1991] analysis of FIRE/SRB experiment treated data from 10 CX pixels and a comparable array of ground sensors deployed over a 100 km spatial scale and averaged on a daily basis over the 17 day experiment. Regression of CX results against surface observations gave slope, intercept, and r^2 of 0.9992, -4 W m^{-2}, and 0.9718, respectively with 9 W m^{-2} standard error at daily resolution. The 17 day mean and standard deviation (in parentheses) based on CX data was 99.7 (±51.8) W m^{-2} and compared with a ground truth value of 103.7 (±51.1) W m^{-2}. The negative bias has been attributed to illumination of the sensors by side lit clouds during the last day of observations [*Whitlock et al.* 1990]. For the C1-based BR2 results interpolated to the center of the sensor array (43.26°N 89.73°W), the slope, intercept, and r^2 were 0.8644, +16.4 W m^{-2}, and 0.9321, respectively. The 17 day mean was 106.0 (± 45.7) W m^{-2}. Although the 17 day mean of the interpolated 280 km C1 data agreed slightly better than CX data with surface observations, the C1 results were significantly worse than CX results in terms of slope, intercept, and 17 day variability. Some but not all of the difference in bias is due to different results for clear sky. The higher intercept and lower slope of the C1 versus surface observations compared to CX statistics is because C1 results generally showed less extreme lows in overcast conditions compared with the CX data. This can be explained by the general occurrence of breaks in clouds and confirms that best results are obtained when the spatial and temporal scales of the satellite and ground observations and the phenomenon studied (clouds) are the same.

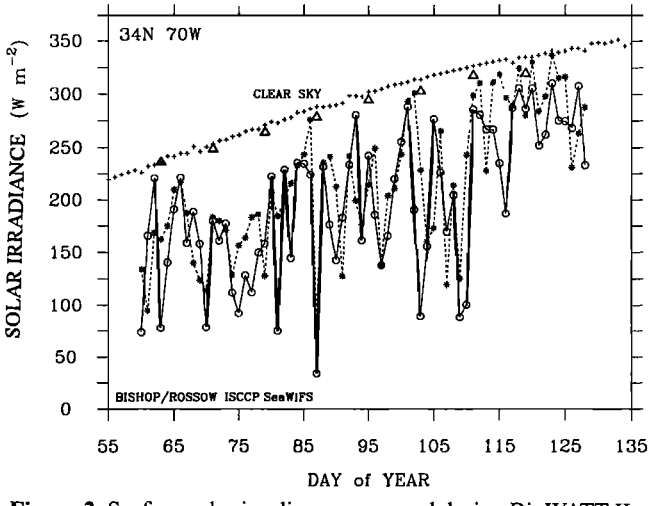

Figure 2. Surface solar irradiance measured during BioWATT II-a versus BR2 ISCCP C1 (280 km) value in 1987. Triangles denote clear sky average from the BioWATT mooring; (pluses) clear sky data from BR2; (circles and solid line) daily average surface irradiance from the mooring; (astersiks and dashed line) daily average irradiance from BR2 data.

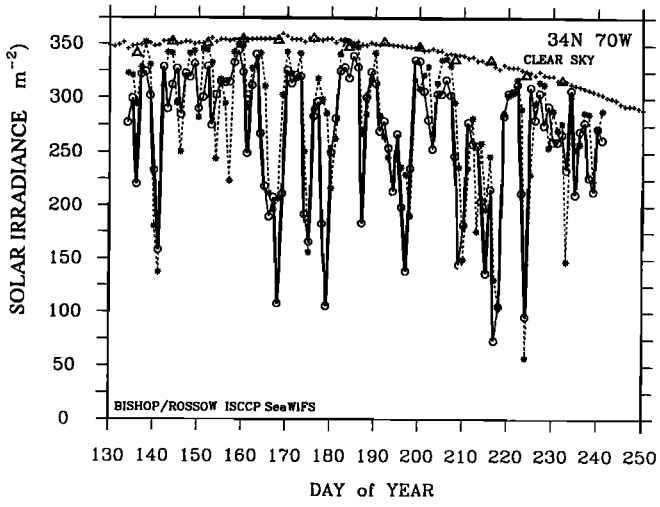

Figure 3. Comparison of the time series of surface solar irradiance measured during BioWATT II-b versus the time series of BR2 ISCCP C1 (280 km) value in 1987. Symbols as in Figure 2.

3.2. Comparison With High-Frequency Contemporaneous Ocean Mooring Observations

Solar irradiance data were obtained from moored sensors deployed in the open ocean during the BioWATT [*Dickey et al.*, 1993] and Marine Light - Mixed Layer (MLML) [*Pluddeman et al.*, 1995] experiments. These experiments, designed to understand physical forcing of biological processes in the ocean, took place southeast of Bermuda and south of Iceland, respectively. Three successive mooring deployments, each lasting approximately 60 days, took place during the BioWATT experiment in 1987 (Figures 2 to 4), and two deployments, lasting 60 days, took place at the MLML site in 1989 and 1991 (Figures 5 and 6). Surface irradiance observations were resolved in time to better than 20 min at the ocean moorings.

The effects of a systematic buoy tilt due to surface currents, if present, could bias clear sky data high or low depending on tilt direction relative to the Sun and is of more concern than effects of random buoy tilts due to wave action [*MacWhorter and Weller*, 1991]. Under overcast conditions, a systematic tilt could allow the sensor to "see" more of a relatively dark ocean and therefore would bias results low. In the case of MLML the surface buoys were very

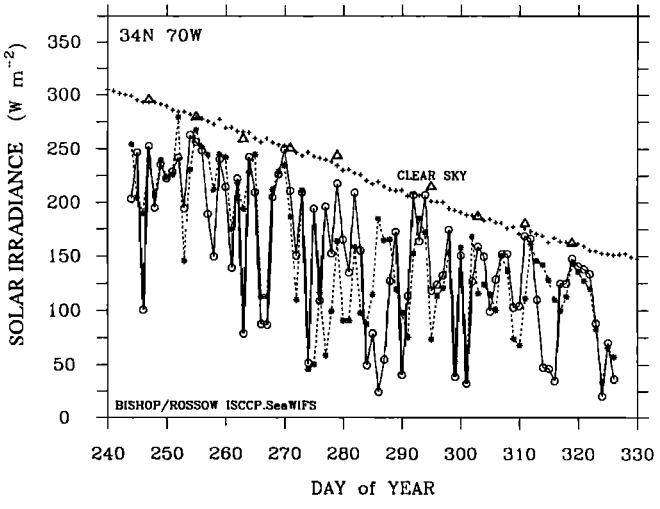

Figure 4. Comparison of the time series of surface solar irradiance measured during BioWATT II-c versus the time series of BR2 ISCCP C1 (280 km) value in 1987. Symbols as in Figure 2.

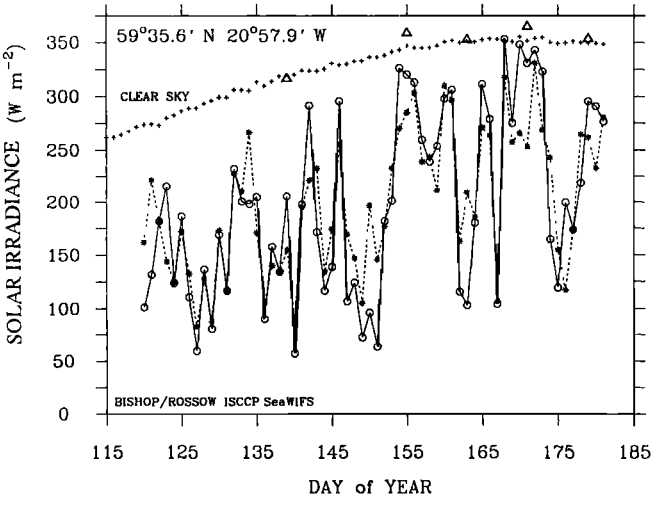

Figure 6. Comparison of the time series of surface solar irradiance measured during MLML II versus the BR2 time series for 1991. Symbols as in Figure 5.

tautly moored with 2000-6000 pounds tension just below the buoy, so pitch and roll was small compared with a ship (R. Weller, personal communication, 1995). Near-surface currents were typically 20 to 40 cm s^{-1} with no consistently preferred direction, and maximum currents rarely exceeded 60 cm s^{-1}[*Dickey et al.*, 1994]. In this way, while a systematic tilt of the sensors due to the action of currents on the buoy is possible, we do not consider it likely. Of the two data sets, those from the BioWATT area near Bermuda should have much less of a bias due to less extreme weather, if a tilt bias exists.

Buoy sensor results are summarized in Tables 1 and 2. In the following we first examine clear sky irradiance in order to evaluate the effects of aerosols, sensor calibration drift or sensor obscuration, and/or buoy motion on the data and then proceed with a comparison of the effects of clouds on surface irradiance at the two sites.

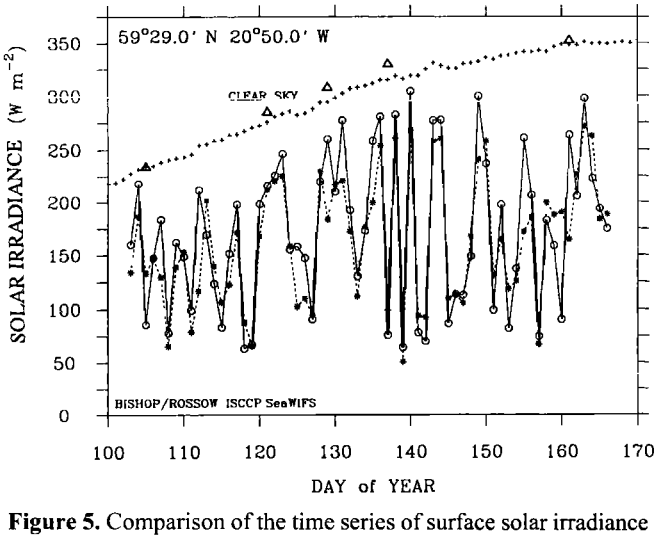

Figure 5. Comparison of the time series of surface solar irradiance measured during the Marine Light Mixed Layer (MLML) deployment I versus the BR2 time series for 1989. Triangles denote clear sky average from the MLML mooring; (pluses) clear sky data from BR2; (circles and solid line) daily average surface irradiance from the mooring; (astersiks and dashed line) daily average irradiance from BR2 data.

Clear sky comparison. Clear sky irradiance was estimated from mooring data by pooling observations over 8 day intervals. Clear sky irradiance is defined as the maximum irradiance recorded over each 10 or 20 minute period, if the ratio of irradiance to cosine solar zenith angle did not change more than 5% compared with the previous reading. This treatment effectively excluded peaks due to anomalous exposure of the sensors by reflection from strongly side-lit clouds. Buoy data were not included in the composite if the observations during a particular period portion fell 10% below the BR2 computed value for clear sky. Inspection of the composite clear sky results showed obvious cloud effects if the latter constraint was not applied. Holes were filled by interpolation. The composite "daily" value was computed for the middle day of the 8 days averaging period and was compared with the BR2 results for the same day. A "daily" clear sky result was not reported for the 8 day period if more than 50% of the integral was based on interpolation

With clear sky values averaged over the 2 month long records, we found differences (BR2 minus mooring) ranging from +7 (BioWATT II-a) to -8 (MLML I) W m^{-2}, suggesting a maximum error of 2.8% in the clear sky model (Table 1). The +7 W m^{-2} average offset in the first BioWATT II record is the combination of an initially good match with BR2 clear sky results in early March 1987 but a 15 W m^{-2} downward drift of the surface observations relative to BR2 by the end of the deployment (Figure 2). This increasing difference during the first deployment may be the result of drift of the buoy sensor's calibration and/or obscuration of the buoy sensor by contaminating agents. The offset vanished in the second and third BioWATT deployments which show offsets of less than 3 W m^{-2}, suggesting that the clear sky records retrieved and the BR2 clear sky data computed from the *Frouin et al.* [1989] formula are in excellent agreement at this site (Figures 3 and 4). Because the MLML site south of Iceland was much more cloudy, we were able to retrieve an 8 day clear sky composite less than 50% of the time (Figures 5 and 6). In this case, BR2 data fell lower than mooring data by 5 and 8 W m^{-2}. Altogether, a weighted average of the 40 clear sky estimates from all five mooring deployments suggest less than 1 W m^{-2} bias.

All-sky records. Daily all-sky irradiance differences averaged over the periods of mooring deployment ranged from +18 (BioWATT II-a) to -9 (MLML I) W m^{-2} with an average bias (standard

Table 1. Comparison of Clear Sky Surface Solar Irradiance Data From BioWATT and MLML Moored Surface Buoys With Data From BR2 (W m^{-2})

Location	Year (Days)	N	Buoy Clear Sky Mean W m^{-2}	BR2 Clear Sky Mean W m^{-2}	Difference BR2-Buoy s.d W m^{-2}	Buoy/BR2
BioWATT II-a	1987 (60-128)	8	282.5	289.6	7.1±5.0	0.9750
BioWATT II-b	1987 (134-241)	13	343.1	344.9	1.7±3.0	0.9948
BioWATT II-c	1987 (244-326)	9	230.0	227.0	-3.0±5.6	1.0132
MLML I	1989 (103-166)	5	301.6	293.4	-8.2±6.1	1.0279
MLML II	1991 (120-181)	5	349.1	343.6	-5.5±7.0	1.0160

MLML, Marine Light Mixed Layer experiment.

deviation in parentheses) of 5 W m^{-2} (± 12 W m^{-2}) (Table 2). The all-sky offsets follow a similar trend as found in the clear sky data. If we normalize the BR2 data by the ratio of clear sky retrieved from the mooring data to BR2 values in attempt to remove possible calibration errors or aerosol effects, then BR2 - mooring differences still average +5 W m^{-2}; however, the standard deviation is reduced to ± 8 W m^{-2}. After normalization the all-sky results indicate less than 5% error relative to clear sky irradiance in the worst case.

Bishop and Rossow [1991] had only one daily resolved time series for comparison; the five new ocean mooring time series add considerably to the validation effort. Generally good agreement was found in temporal variability of surface irradiance retrieved by satellite and recorded by the buoy-mounted sensors. The coherence between the BR2 retrieved and BioWATT recorded data (Figures 2-4) broke down occasionally for 1 or 2 days when the two data sets show opposite trends or lags or leads (e.g., Figure 2, days 75-80 and days 102 -107). At the MLML site, the buoy sensor and satellite data track each other much better (Figures 5 and 6). This is probably due to the different phases of weather systems captured in a 280 km pixel versus a single point.

Regression of the 387 individual daily surface irradiance observations from the five deployments versus BR2 data (Figure 7, top) yields results far worse than that reported by *Bishop and Rossow* [1991] for the FIRE/SRB experiment. In this case, a slope of 0.82, intercept of +42 W m^{-2}, r^2 of 0.71, and standard error of 43 W m^{-2}, were obtained. As already discussed, BR obtained a slope of 0.999, intercept of -3.7 W m^{-2}, r^2 of 0.972, and standard error of 9 W m^{-2} for the FIRE/SRB effort over land where satellite pixels (CX) and sensors were matched on similar spatial scales (both 100 km scale). The comparison with BR2 data from C1 (100 km versus 280 km scales) yielded less satisfactory results. The current analysis compares point observations with areal averages over a 280 km x 280 km box. This mismatch of spatial scales yields amplified differences seen in the correlation and time series of data. For example, the areal mismatch also is reflected in the standard deviations of the two data sets; the highs and lows of the BR2 data sets (Figures 5 and 6) are generally less extreme due to averaging of meteorological conditions over the 280 km sized pixel. When we averaged both the BR2 and the buoy data over 5 days, a timescale more typical of synoptic weather disturbances, correlation between the two data sets improved significantly (Figure 7, bottom). Results gave a regression slope of 0.99, intercept of 9 W m^{-2}, and r^2 of 0.86. Most importantly, the scatter is reduced from 43 W m^{-2} for the daily data to 24 W m^{-2} for the 5-day-averaged data.

Rossow and Zhang [1995] report similar studies of sampling effects on comparisons of surface with satellite fluxes; they show a similar improvement in the comparisons when results are averaged over larger samples either in time or over an area. Since solar insolation varies most because of changes in cloudiness, the study of *Seze and Rossow* [1991] is also relevant: they show that the sparse ISCCP sampling of cloud variations over the 280 km spatial scale still represents the areal mean properties relatively well.

3.3. Comparison With High-Frequency Contemporaneous Ocean Island Observations

The BioWATT and MLML experiments lasted for relatively short durations. To examine the long-term behavior of the solar irradiance data over maritime regions, we turned to several long time series for oceanic island sites. The comparison also allowed examination of the BR2 irradiance data across the transitions among NOAA 7, 9, and 11 satellites (Appendix section A1). Irradiance data sets resolved in time to better than 60 minutes were obtained from Samoa (1983-1991), Kwajalein (1989 to 1991), and Bermuda (1990-1991) using the same protocols and personnel under the direction of one of us (EGD) as part of NOAA's program for climate monitoring [*Bodhaine et al.*, 1993]. The sensor at Ber-

Table 2. Comparison of Surface Solar Irradiance Data From BioWATT and MLML Moored Surface Buoys With Data From BR2 (W m^{-2})

Location	Year (Days)	Buoy Mean ±s.d. W m^{-2}	BR2 Mean ±s.d. W m^{-2}	BR2 Mean (Normallized)	Difference BR2-Buoy W m^{-2}	Error percent of Clear Sky	Difference BR2-Buoy Normallized	Error percent of Clear Sky
Biowatt II-a	1987 (60-128)	197.6±69.6	215.5±60.2	210.1	+17.9	6.3	+12.5	4.4
Biowatt II-b	1987 (134-241)	265.9±62.5	280.7±51.7	279.2	+14.8	4.3	+13.3	3.9
Biowatt II-c	1987 (244-326)	148.9±66.2	147.4±56.4	149.3	-1.5	-0.7	+0.4	0.2
MLML I	1989 (103-166)	172.9±71.2	164.1±59.3	168.7	-8.8	-2.9	-4.2	1.4
MLML II	1991 (120-181)	197.9±86.4	200.0±60.4	203.2	+2.1	0.6	+5.3	1.5
Average					4.9±11.2	1.5±3.7	5.5±7.6	2.3±1.8

Normallized: uses Table 1 clear sky (buoy/BR2) ratio to adjust data for possible differences in calibration/aerosol effects.

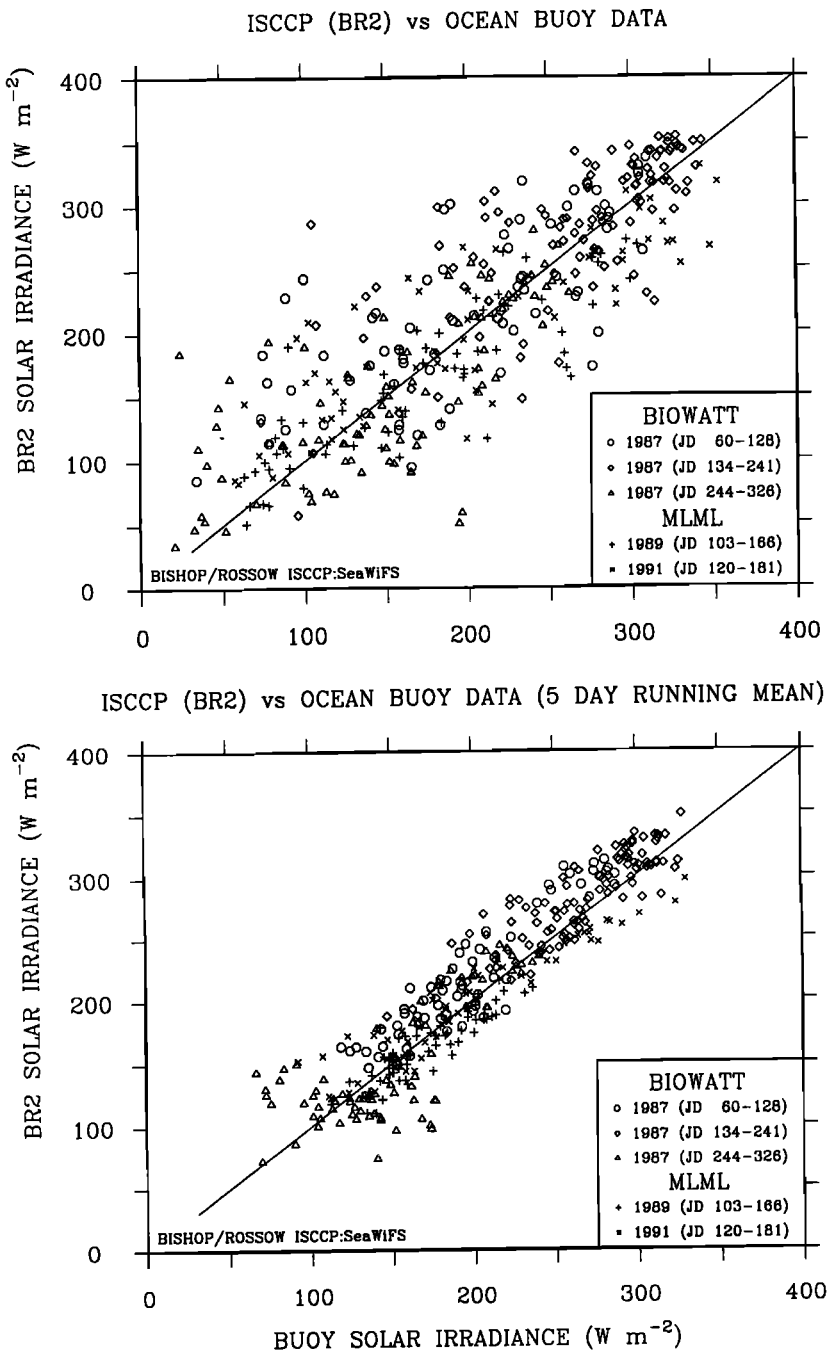

Figure 7. Regression of surface solar irradiance measured at ocean buoys versus contemporaneous BR2 data for (top) daily averages; and (bottom) 5-day averages. BioWATT: (circles) 1987, days 60-128; (diamonds) 1987, days 134-241; (triangles) 1987, days 244-326; MLML: (pluses) 1989, days 103-166; 1991, days 120-181. A line of slope 1 is drawn for reference.

muda was destroyed before it could be recalibrated. Data for Cape Grim (1985-1991), Australia, were obtained courtesy of B.W. Forgan, Bureau of Meteorology, Australia. The NOAA observations are referenced to the World Radiation Reference scale maintained by the World Meteorological Organization (WMO) in Davos, Switzerland, and are believed to be accurate to ± 2% or 5 W m^{-2}, which ever is largest, when averaged over time periods of a day or longer in the tropics. The Samoa and Cape Grim records were also used in the *Cess et al.* [1995] analysis of the effects of clouds on surface solar irradiance. Of the several locations used in their analysis, over 85% the data came from Samoa, Cape Grim, and Wisconsin (FIRE/SRB experiment).

Although sensor calibration protocols were rigid, we recently did discover data processing errors in both the Samoa and the Cape Grim surface data sets. Our analysis of the Samoa data for local noon from July 1983 to June 1991 revealed an error that caused the month of December 1986 and all of 1987 to be 13% high relative to the rest of the record and to exceed our clear sky estimate by a similar amount. This anomalous period, where fortuitously good agreement with monthly averaged BR2 data was found (Figure 8, bottom), was referred to by *Cess et al.* [1995] as influenced by anomalous cloud conditions associated with El Nino and thus eliminated from their analysis. After the data processing problem was identified and corrected, the discrepant data fell in line with the rest

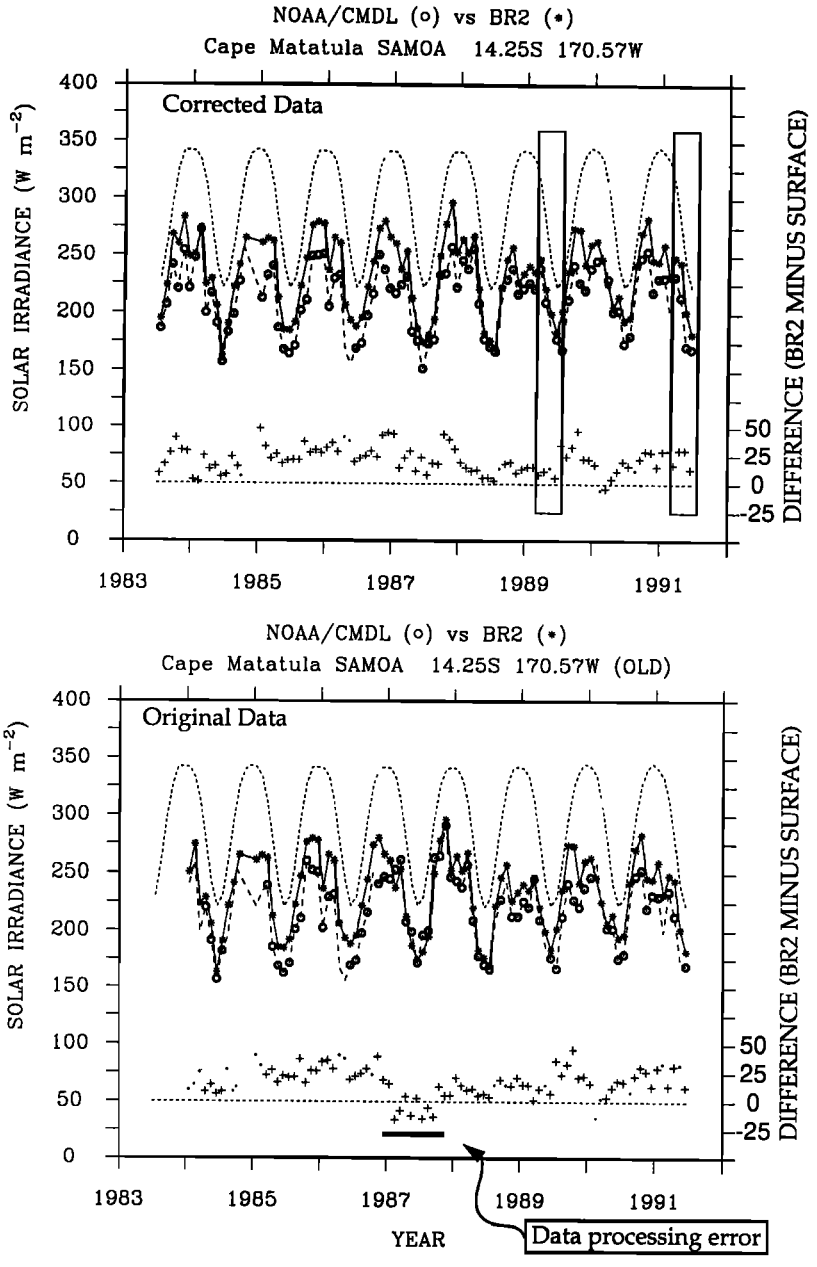

Figure 8. Comparison of the time series of monthly mean surface solar irradiance measured at Cape Matatula, Samoa (circles and dashed line), and the BR2 monthly means (astersiks and solid line) using the corrected data (top) and original uncorrected data (bottom) for Cape Matatula. The upper dashed line represents the monthly mean clear sky solar irradiance from the BR2 algorithm. Both plots: (pluses) Irradiance difference (BR2 minus surface observations) plotted relative to the right-hand scale. Daily data from boxed areas are shown in Figure 12.

of the record, namely BR2 data were approximately 20 W m^{-2} higher than surface observations at Samoa. The problem with these data was not with the instruments or their calibration but in the data reduction process.

A data problem in the opposite sense was identified in the Cape Grim data (Figure 9). In this case, the BR2 and surface data spanning the period 1985 to 1989 were offset by approximately 15% (BR2 data high); however, data from June 1990 onward agreed almost perfectly. Our analysis of this data set showed that the clear sky envelope of the surface observations fell consistently low by 15% compared with BR2 calculations for the 1985 to mid-1990. Furthermore, the transition from bad to good agreement coincided exactly with installation of a new sensor in June 1990. The correction to the data involved multiplying the erroneous 1985 to 1989 surface observations by 1.1493 (B.W. Forgan, personal communication, 1995). The corrections mentioned here have been applied to the data now available from the Cape Grim site; the data for February through May 1990 are unlikely to be recoverable. The deviations in corrected data for early 1987 do not appear to be related to instrumentation or data processing problems.

We infer that data errors of similar nature may contribute to other data sets of solar irradiance, such as the extensive monthly mean data in GEBA (discussed later); however, our experience shows that it is impossible to discover 10-20% errors (as detected above) based on monthly means alone.

At Cape Grim the 25 W m^{-2} bias inferred by our first comparison

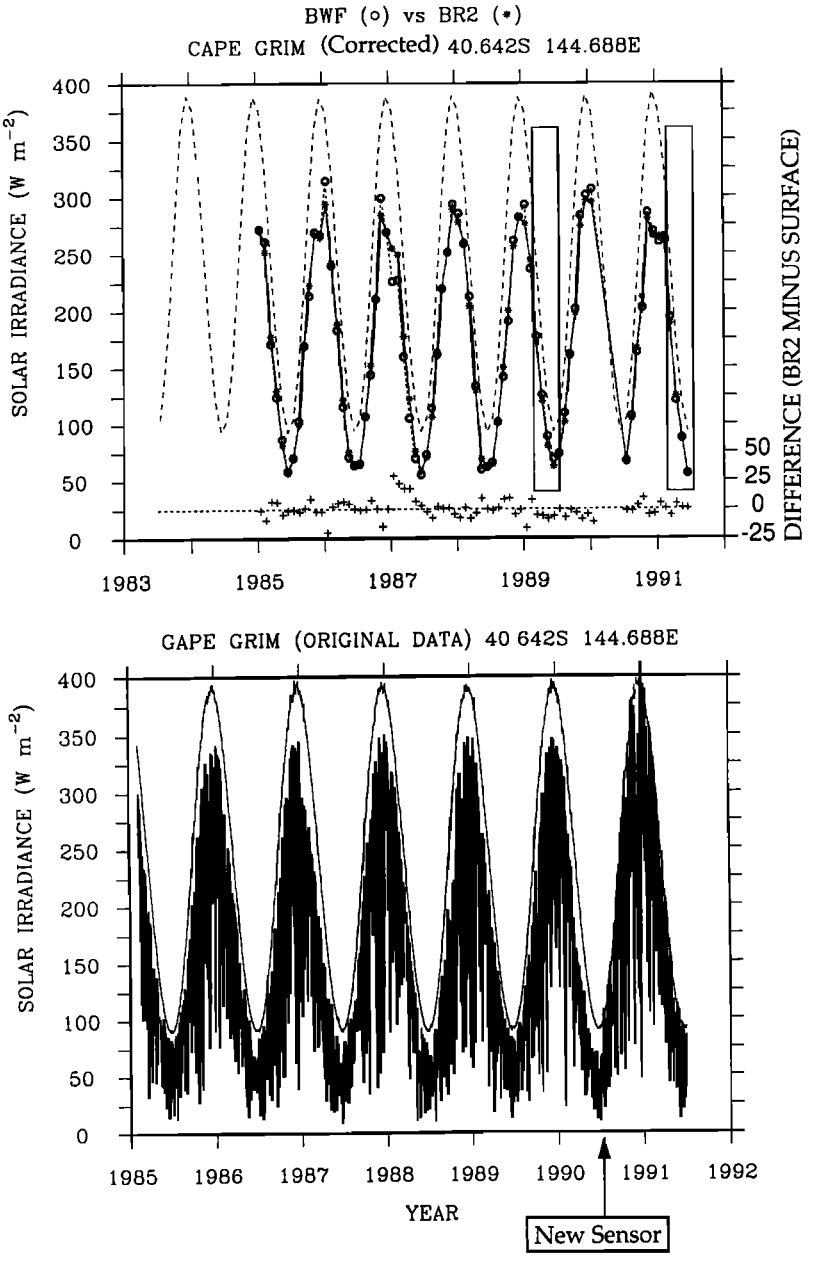

Figure 9. (top) like Figure 8 but for Cape Grim, Australia. (bottom) daily averages of Cape Grim surface observations (BWF) versus BR2 clear sky in the uncorrected data set. The upper envelope of the surface observations matched closely BR2 clear sky results (upper dashed line) from June 1990 onward, the date of installation of a new sensor (see text). The data currently available from Cape Grim are correct and reflect the multiplication of the older pre-February 1990 results by a factor of 1.1493.

was an artifact of a data error. The 25 W m^{-2} bias reported by *Cess et al.* [1995] for Cape Grim was also based on incorrect data. BR2 data versus corrected data over 73 months have a bias of 0 W m^{-2} and a standard deviation of ±8 W m^{-2} with little consistent seasonality. A comparison of other satellite surface radiation retrievals for 46 months from 1985 to 1989 using the Pinker and Staylor algorithms [*Pinker et al.*, 1995] with Cape Grim surface observations also gave low annual mean differences (± monthly standard deviations) of -2.9 (± 9.7) and -0.9 (± 13.4), respectively. The seasonal trends of differences have larger amplitudes than for BR2 retrievals at this location (Figure 10). The validation results at Wisconsin reported by *Bishop and Rossow* [1991] show a bias of less than 5 W m^{-2}. In the single case of Samoa, the correction of data did result in a more consistent offset of approximately +20 W m^{-2} between BR2 and surface observations over the entire record examined leading us to examine in greater detail the tropical data sets. Whatever the case, the data investigated do not support the conclusions of *Cess et al.* that a +25 W m^{-2} bias is a global phenomenon.

3.4. Ocean Island Observing Sites

We have seen that observations at Cape Grim agree within a few W m^{-2} of satellite estimates on an annual basis. BR2 data from Kwajalein atoll (Figure 11) is biased high by 10 W m^{-2}, only half

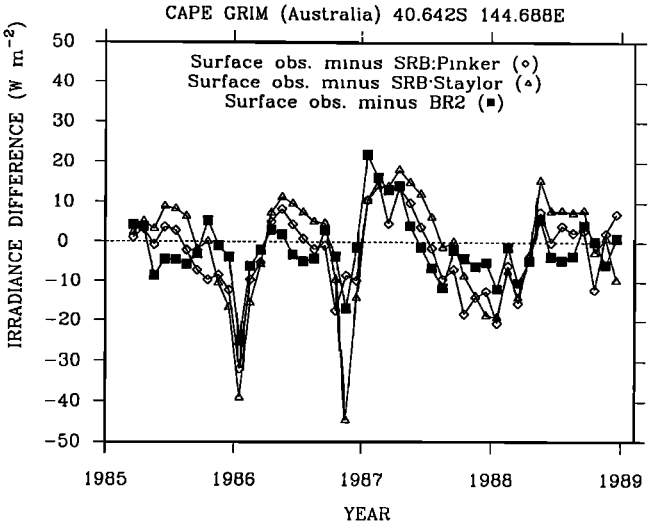

Figure 10. Comparison of satellite-based data sets versus surface observations at Cape Grim March 1985 to November 1988. Diamonds and triangles from Pinker and Staylor algorithms [*Pinker et al.*, 1995]; and solid squares from the BR2 method. All data sets have an annual mean difference from surface observations amounting to less than 2 W m^{-2}. BR2 estimates show less seasonality in difference compared to the other two methods at this location.

of the bias seen at Samoa. The short data record from the island of Bermuda are in excellent agreement during months of October 1990 through January 1991 but disagree by as much as 40 W m^{-2} in the early summer 1991. A key to these differences may lie in the siting of sensors on the coastal/island locations and meteorological effects on the local scale of the sensors.

Cape Grim, Tasmainia, has an immediate (20 m) western exposure to the southern ocean and is 2 km from the Bass Strait to the north. Its location is dominated by ocean winds and sky conditions. Samoa (88 km^2 in area and maximum elevation of 660 m) is significantly larger and more elevated than the atoll island of Kwajalein (3.1 km^2 area and maximum elevation of 10 m). Cape Matatula, the location of the sensor on Samoa, is found on the eastern extremity of the island and was chosen because of its exposure to the prevailing winds. At Samoa, orographic clouds can be seen on occasion at a distance of 5 to 10 km from the station, directly to the west. Bermuda is intermediate in size between Samoa and Kwajalein and has generally low topography but several large lagoons. The Bermuda observing site is located on the NE side of the island. The differences seen in at Bermuda (Figure 11) may be the result of micro and mesoscale meteorological effects caused by the size of the island and the specific site of the observing station. This is examined in more detail below.

Kwajalein versus Samoa records of daily irradiance. We selected four months of daily averaged data (March through June) from the Samoa and Kwajalein surface observations from 1989 and 1991 to further analyze causes of disagreement between surface and BR2 data. These island locations are compared because they are both tropical, have similar levels of cloudiness, yet they have vastly different topography and size.

Figures 12 and 13 show the daily averaged all-sky irradiances as calculated by BR2 data and as measured for the two island locations. Clear sky irradiances from BR2 are used as a reference for the two data sets since clear sky irradiances could not be extracted from the surface observations because of their 1 hour averaging period. Relative to the BR2 clear sky surface insolation, the reduction of solar irradiance by clouds (and aerosols) estimated from BR2 data was 85% and 65% of that recorded by the sensor at Samoa (Table 3) for the two 4 month records for 1989 and 1991. One would be tempted to use the term "cloud forcing" to describe these percentage differences, but our numbers also include aerosol effects which are currently unquantified. The corresponding values for Kwajalein for 1989 and 1991 were 89% and 82%, respectively. A similar comparison at Bermuda (32° N, 65° W; Table 3) shows that the BR2 cloud attenuation was 69% relative to that observed for 1991. By contrast, in the nearby sub-tropical Atlantic at the BioWATT site (34° N 70° W), BR2 yielded cloud (and aerosol) attenuation that is much better agreement with observations. In this case, relative percentages ranged from 77 to 99% for the three separate buoy deployments.

We do not believe that the differences between Samoa and Kwajalein can be explained simply by variations in atmospheric transmissivity between these two sites, since the upper envelopes of BR2 and surface observations are in good agreement. Furthermore, the aerosol optical thickness index climatology of *Stowe et al.* [1992] over oceans shows no discernible difference between the two sites. For both sites, including a better estimate of aerosol effects on atmospheric transmissivity, could reduce the magnitude of differences by approximately 10 W m^{-2} and thus completely eliminate the offset at Kwajalein. Our analysis shows, however, that the largest differences occur on cloudy days. For example, in the 1991 daily record from Samoa the underestimate of solar irradiance by BR2 on some of the cloudiest days is as large as 100 W m^{-2}. It is these rare events which contribute significantly to the monthly mean differences. Interestingly, the timing of cloudy events at Samoa was consistent in both BR2 and surface records, so the differences are not due to events missed by the satellite but due to enhancement of the magnitude of the events in the sensor records compared with BR2 retrievals. We note again the better consistency of the two kinds of records at Kwajalein. It is unlikely that differences in satellite calibration can explain the relatively poor results at Samoa but relatively good agreement at Kwajalein since the same satellite was used for the observations.

Bermuda. The poor agreement between surface observations and BR2 data in the spring and summer 1991 was a surprise since the topography of Bermuda is much more akin to Kwajelein. In May 1996, EGD observed a stationary cloud aligned with the island along the northeastern side of the island complex. It turns out that there is a phenomenon known to local meteorologists as "Captain Morgan's cloud" [*Zuill*, 1946]. This complex is best developed with light winds up to 600 mbar with weak to stronger vertical instability and light steady winds from the SW; it is present generally from mid-April to September. When the cloud is moderately developed, it would shade the pyranometer; however, its small size would fail to impact cloud retrievals at the ISCCP C1 280 km scale. Thus the sense and seasonality of the difference due to Captain Morgan's cloud matches the sense of our comparisons almost exactly even though we cannot make a quantitative estimate of its impact on our comparison.

Sensitivity to calibration errors. In order to examine the sensitivity of surface irradiance data to errors in calibration, we ran the BR2 scheme for two 4 month periods in 1989 and 1991 with cloud radiances adjusted upward by 15%. This correction is bigger than the 12% adjustment already made to the NOAA 11 radiances (Appendix A1). The choice of 15% was based on the *Frouin et al.* [1995] suggestion that ISCCP radiances may be biased 15% low. Results from our revised calculations are presented in Table 3.

The adjusted time series show significant improvement for

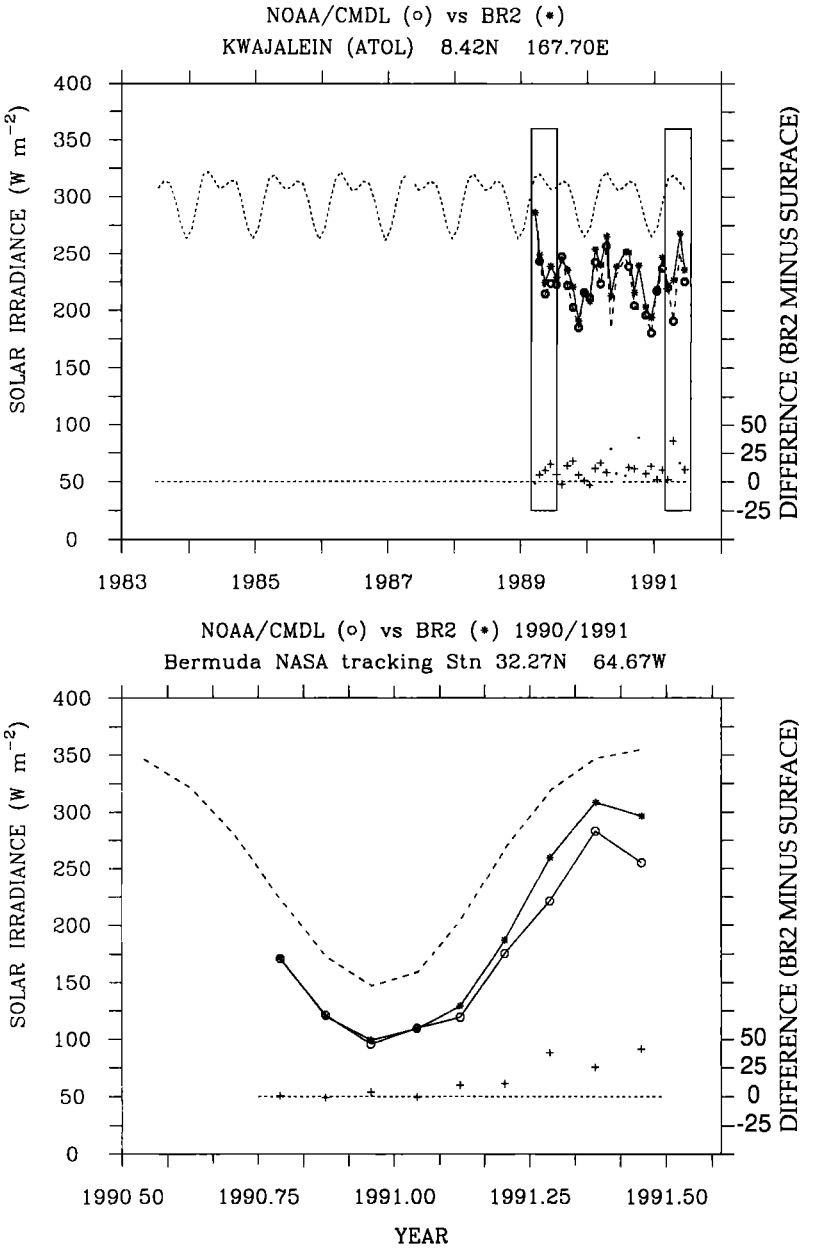

Figure 11. Comparison of the BR2 monthly mean time series (astersiks and dashed line) and the time series of surface solar irradiance measured at Kwajalein atoll (circles and solid line) (top), and at at Bermuda (circles and solid line) (bottom). The upper dashed line above the two data sets represents the clear sky solar irradiance modeled by BR2.

Kwajalein and partial improvement for Samoa. After adjustment, BR2 estimates of the reduction of surface irradiance by clouds relative to that in surface observations for early 1989 and 1991 are 99% and 77% for Samoa and 104% and 97% for Kwajalein, respectively. Similarly, 1991 data for Bermuda showed cloud attenuation was 69% of surface observations before and 81% after adjustment. The daily records for Bermuda before and after adjustment (Figure 14) show that it is neither sensor calibration nor aerosol effects that contribute most to the disagreement; it is the fact that cloud events are more intensely seen in the surface observations. We note also at the MLML site south of Iceland that the comparative cloud attenuation ratios changed from an excellent 100% and 95% for 1989 and 1991, respectively, to 115% and 109% for the same two years after the +15% radiance adjustment. For Cape Grim the ratios change from 85% and 98% for unadjusted data to 97% and 112% after adjustment for the same two years. Of interest is the fact that the MLML data sets which agreed well move into poor agreement. This lack of global consistency and the problems with data at Bermuda and Samoa suggests that something besides satellite calibrations explain the differences presented above.

We suggest that the location of sensors on islands and the size of islands can strongly influence the degree of agreement or disagreement of the data. At coastal locations, clouds tend to form over land when land is warmer than the ocean and over the ocean when land is cooler than the ocean. This is well documented as a response to sea / land breezes diurnally and to monsoons on seasonal and longer timescales. There is the navigator's rule of thumb for the tropics that land may be identified by the occurrence of convective clouds in the afternoon. The much greater size of Bermuda and Samoa and the east-coast location of the sensors in comparison

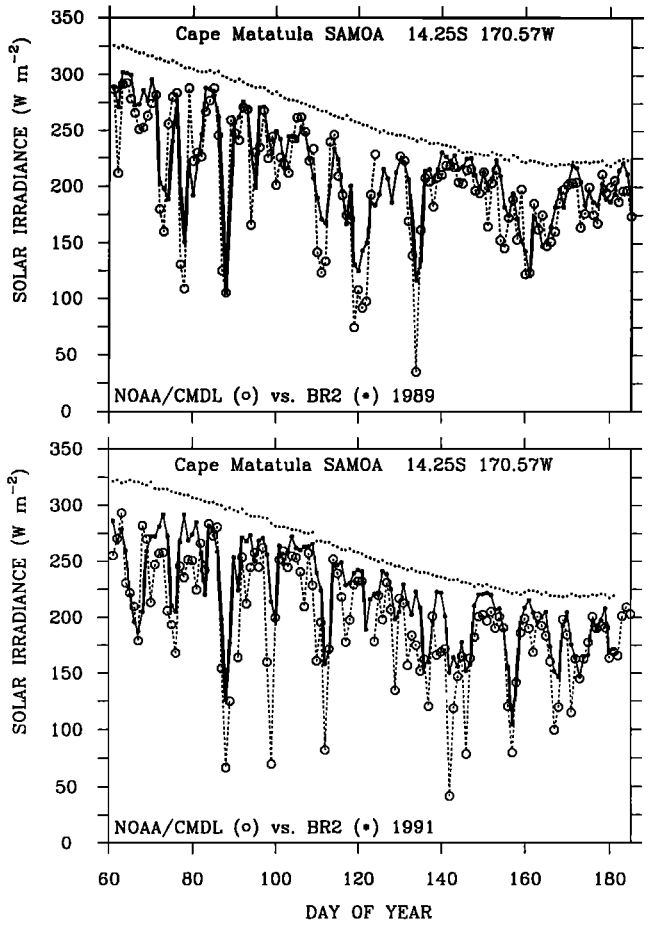

Figure 12. Comparison of the daily-mean surface irradiance measured at Cape Matatula, Samoa (circles) and the daily-mean BR2 (astersiks) data for (top) 1989 and (bottom) 1991. The small pluses represent the daily averaged clear sky solar irradiance modeled by BR2.

with Kwajalein suggest that microscale and mesoscale meteorology plays a significant role in exaggerating the differences between satellite and ground observations. In this way, we argue that the BR2 data, with a 280 km spatial resolution, is more representative of the solar irradiance on that scale over the oceans than data from large islands.

3.5. Comparison at High Spatial Resolution

As one of the steps in the production of 30 km data SeaWiFS, we have produced 5 days (March 1 to 5, 1991) of surface irradiance data at 0.5° (55 km maximum spatial resolution) using the new ISCCP DX product. Using a 5 min. topography database, we selected the highest elevation within the 0.5° grid box. This allowed us to preserve islands smaller than 0.5° in size. Predominantly island locations were identified by having four or more immediately adjacent pixels (of eight possible) with bathymetry greater than 100 m. The average surface irradiance of the surrounding water pixels was then subtracted from that of the identified "island" point. Land minus ocean differences were binned in 20° latitude bands and presented as histograms (Figure 15). Overall, solar irradiance differences ranged from -65 to +85 W m^{-2}, and majority of data from 10°N to 10°S in the tropics were skewed below zero. On average, land points were biased 4 W m^{-2} lower than the surrounding ocean in this band. This lends support to the notion that surface irradiance data from tropical island locations are not representative of the surrounding oceanic waters. Data from more polar regions suggest less (or opposite) negative bias consistent with more cloudiness over the oceans than over ice. A longer time series would probably yield the same results given the fact that 5 days time is sufficient to average out the effects of subgroup scale weather systems (see, for example Figure 7).

3.6. Comparison With Contemporaneous GEBA Climatology

Some 500 surface stations with 2 or more years of contemporaneous data were selected from those present in the Global Energy Balance Archives (GEBA), [*Ohmura et al.*, 1991]. The data and data quality are not well documented although major effort is being made to address this problem. Our experience suggests that errors like those found in the Samoa and Cape Grim data sets may be hidden within the monthly means on file with GEBA. The following analysis therefore makes an unsubstantiated assumption that the surface observations are "truth,"

The BR2 surface irradiance data, Q_{TOT}, and clear sky data, Q^*_{CLR}, have been interpolated to the locations of all stations present in the archives. Because surface elevations at individual stations on land do not match the mean elevation corresponding to the 280 km sized C1 pixel, a small adjustment in BR2 irradiance is made on the basis of computed surface pressure differences as follows:

$$Q'_{TOT} = Q_{TOT}(e^{-(0.073/\mu(p\text{GEBA}/1000))})/(e^{-(0.073/\mu(p\text{C1}/1000))}) \quad (1)$$

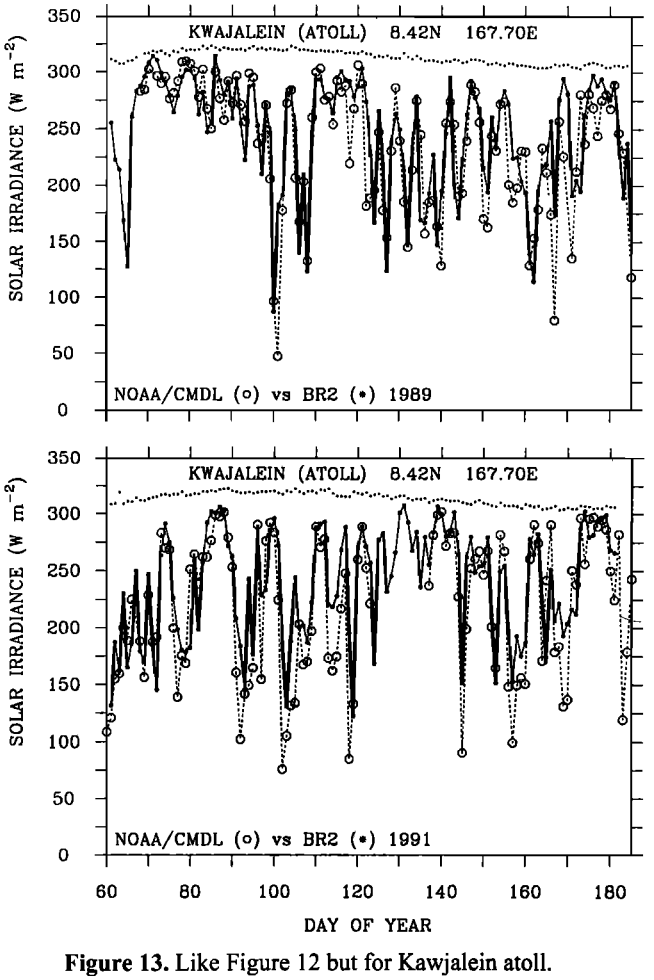

Figure 13. Like Figure 12 but for Kawjalein atoll.

Table 3. Comparison of Surface Solar Irradiance Data From BioWATT and MLML Moored Surface Buoys, and High Quality Surface Observations with BR2 data (W m^{-2})

Location	Year (Days)	N Days	BR2 Clear Sky	Mean ±s.d. SOBS	Mean ±s.d. BR2	Mean ±s.d. +15% BR2	Difference BR2 - SOBS	Difference BR2 - SOBS (+15%)	Cloud Forcing* (Clear Sky minus All sky) SOBS	Cloud Forcing* (Clear Sky minus All sky) BR2	Cloud Forcing* (Clear Sky minus All sky) BR2 (+15%)
MLML*	1989 (103-166)	64	302.7	172.9±71.2	164.1±53.1	144.8±58.5	-8.8	-28.1	138.2	138.6	157.9
60°N 21°W	1991 (120-181)	62	328.4	197.9±86.5	198.0±60.4	179.0±67.2	+0.1	-18.9	135.8	128.4	149.4
Biowatt II*	1987 (60-128)	69	294.9	197.6±69.6	215.5±60.2	nd	+17.9	nd	102.6	79.4	nd
34°N 70°W	1987 (134-241)	108	342.6	265.9±62.5	280.7±51 7	nd	+14.8	nd	75.3	61.9	nd
	1987 (244-326)	83	222.2	148.9±66.2	147 4±56 4	nd	-1.5	nd	75.2	74.8	nd
Bermuda	1989	nd	nd	nd	nd	nd	nd	nd	nd	nd	nd
32.3°N 64.7°W	1991 (60-181)	115	320.0	231.2±79.3	258.9±64.1	248.4±69.2	+27.7	+17.2	88.8	61.1	71.6
Kwajalein	1989 (60-180)	114	314.1	239.5±56.1	246.7±50.8	236.1±59.3	+7.2	-4.5	74.6	66.4	78.0
8.42°N 167.7°E	1991 (60-180)	109	313.5	218.2±62.5	235.1±49.5	221.1±58.7	+16.9	+2.9	95.3	78.3	92.4
Samoa	1989 (60-180)	108	263.1	205.1±52.4	215.1±43.8	204.8±48.1	+10.0	+0.3	58.1	48.1	58.4
14.25°S 170.57°W	1991 (60-180)	112	261.5	196.0±51.7	218.8±42.4	211.5±45.3	+22.7	+15.5	65.5	42.7	50.0
Cape Grim	1989 (60-180)	120	159.0	98.4±49.7	107.5±50.0	100.1±49.1	+9.1	+1.7	60.6	51.5	58.7
40.64°S 144.69°E	1991 (60-180)	116	161.9	115.0±61.7	115.8±56.2	109.3±55.0	+0.8	-5.7	46.9	46.1	52.6

* Surface observations normallized using data in Table 1. nd, not done; N Days, number of days in average; SOBS, surface observations.

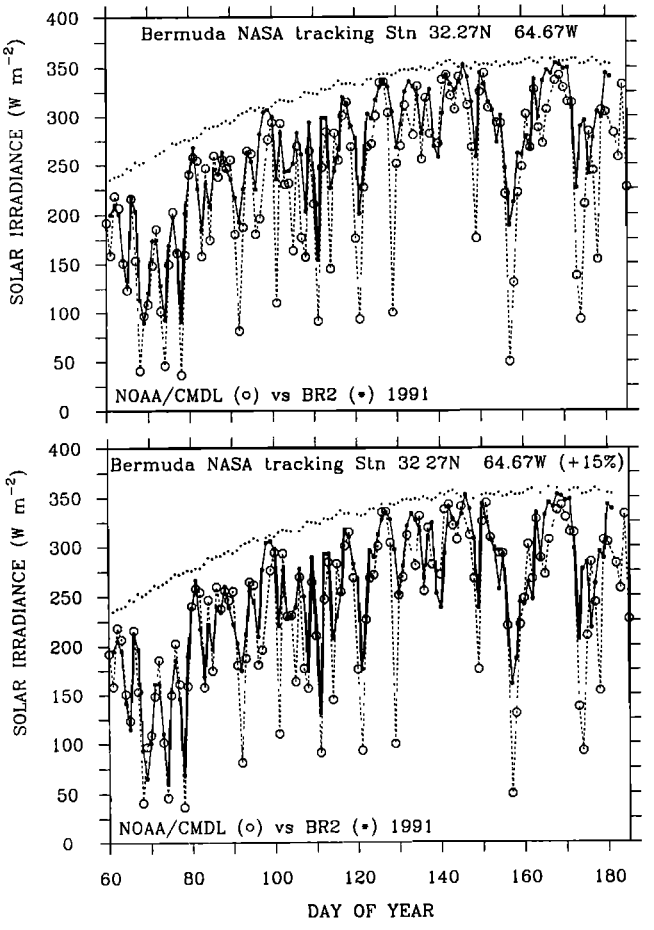

Figure 14. Like Figure 12 but for Bermuda. (top) 1991 data. (bottom) 1991 data recalculated after adjusting ISCCP radiances upward by 15%.

where 0.073 is the combined effect of atmospheric scattering and aerosols from the *Frouin et al.* [1989] formula, μ is the flux weighted cosine of solar zenith angle, and *p*GEBA and *p*C1 are the surface pressures computed for the GEBA station and from the C1 data in hectopascals. The resulting corrections adjusted data by less than 2% but did improve the comparison. The plot of all station matches (some 21,000 data pairs) is shown in Figure 16. Linear regression statistics gave

$$Q'_{TOT} = 1.090 \pm 0.003\ (Q_{GEBA}) + 4.5 \pm 0.6\ \text{W m}^{-2};$$
$$\sigma_y = 23\ \text{W m}^{-2};\ r^2 = 0.940. \quad (2)$$

This result and examination of the data show that BR2 data overestimate surface irradiance at some stations by as much as 50 - 100 W m^{-2}. Because the latitudinal distribution of stations is uneven (65% of stations are found between 30°N and 60°N), we have chosen to characterize the differences locally in terms of an atmospheric optical extinction anomaly (τ*) required to bring the BR2 data into agreement with surface observations:

$$Q_{GEBA} = Q'_{TOT}\, e^{(-\tau^*/\mu)} \quad (3)$$

where μ is the flux-weighted cosine of solar zenith angle of the day at midmonth; Q_{GEBA} is the monthly averaged surface observation.

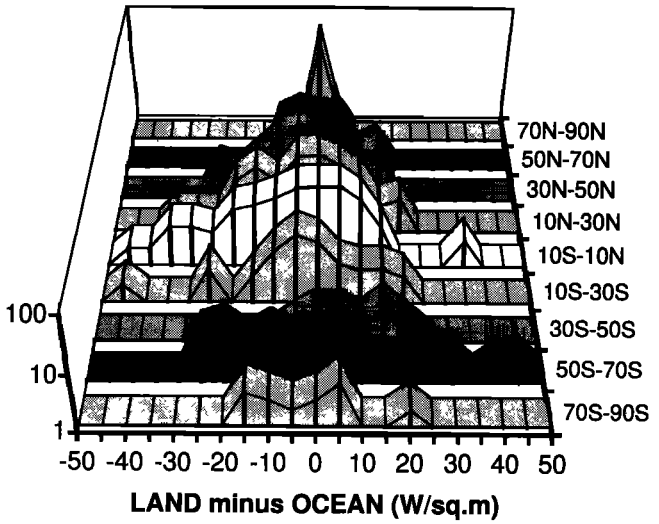

Figure 15. Histogram of the difference in surface solar irradiance of island/coastal and surrounding waters for different latitude zones. Locations were selected by having four or more adjacent ocean pixels. The data are from the surface solar irradiance retrieved by the BR2 scheme using high-resolution (0.5°) ISCCP DX data for March 1-5 1991.

A positive τ^* means an overestimate of surface solar irradiance in the BR2 calculation.

Bishop and Rossow [1991] held aerosol effects constant both in time and in space with an effective atmospheric extinction coefficient of 0.014 (aerosol optical thickness ~0.04), and the same assumption has been made for BR2 data. These low values do not apply for dusty or polluted continental environments, nor in oceanic environments influenced by mineral or anthropogenic aerosols, nor in the presence of volcanic aerosols such as derived from the recent eruption of Mount Pinatubo. As discussed previously, it is impossible to separate contributions of errors in the clear sky model or ground observations, errors in our treatment of aerosols, or the errors in cloud radiative transfer parameterization using monthly mean data. Thus our atmospheric optical extinction anomaly is a measure of all the errors.

An example of the computation of atmospheric extinction anomaly and its interpretation is illustrated for two pairs of neighboring coastal points from the GEBA data set. These stations were chosen since they are representative of "bad" and "good" agreement and illustrate the importance of local processes in contributing to differences. Furthermore, we wish to provide a better context for seasonal analysis of extinction anomaly pattern on a global basis.

Hong Kong (863) and Macau (912), located in the far western Pacific near 22°N, 114°E, are separated by only 65 km. Both show up to 100 W m^{-2} (τ^* up to 0.6) differences between BR2 retrievals and surface observations in months of March and April in a repeating pattern over the 4 year time series (Figure 17). Annual mean biases average +46 and +30 W m^{-2} at these two stations, respectively. Both stations are known to be under the influence of continentally derived mineral dust aerosols in the springtime; however, anthropogenic effects are readily seen in summertime data at Hong Kong. Anthropogenic aerosols may explain differences as large as 60 W m^{-2} (τ^* = ~0.2) which persist throughout the summer months at Hong Kong but are much reduced (τ^* = <0.1) at the less industrialized Macao (Figure 17). Cape St. James (431) and Sandspit (433), separated by 155 km, are located in the temperate NE Pacific at the southern tip and on the east coast of the Queen Charlotte Islands, off the west coast of Canada. Both locations show much better agreement between BR2 data and surface observations than Hong Kong and Macao. Cape St. James, being well exposed to westerly winds from the Pacific (and facing equatorward toward the Sun), shows τ^* values which rarely exceed 0.05, an annual bias of -0.5 W m^{-2}, and a monthly bias of less than 10 W m^{-2}. Sandspit on the sheltered east coast of the island shows an annual bias of +11 W m^{-2} with up to +36 W m^{-2} differences in the summer. The differences between the exposed Cape St. James and sheltered Sandspit locations could be due to a systematic increase of cloudiness to the west of the sensors in the afternoons due to the local land/sea breeze circulation as well as to greater contributions from aerosols from biomass burning (related to the forest industry) or natural forest fires in the dry summer months. In every case, BR2 and surface observations agree best during the winter months November through January. This is consistent with our general observation that most GEBA stations agree best in the wintertime.

Global optical extinction anomaly (τ^*) maps derived from GEBA and BR2 data and contoured at 2.5° resolution (Plate 1) depict averages for the four seasons: winter as December, January and February (DJF); spring as March, April, May (MAM); summer as June, July, August (JJA); and fall as September, October, and Novvember (SON). Also included on the maps are τ^* data for Samoa, Kwajalein, and Cape Grim (see section 3.3). For comparison, seasonally mapped distributions of aerosol optical thickness index (at 1° resolution) derived for the ocean from AVHRR data are shown for the years July 1989 to June 1991 (Plate 2) [*Stowe et al.* 1992]. We use the Stowe data as an index since its relationship to aerosol optical thickness is systematic but not calibrated. Since most of the GEBA-BR2 matchups of data occur in the middle to late 1980s, the Stowe et al. data sets are not contemporaneous; they

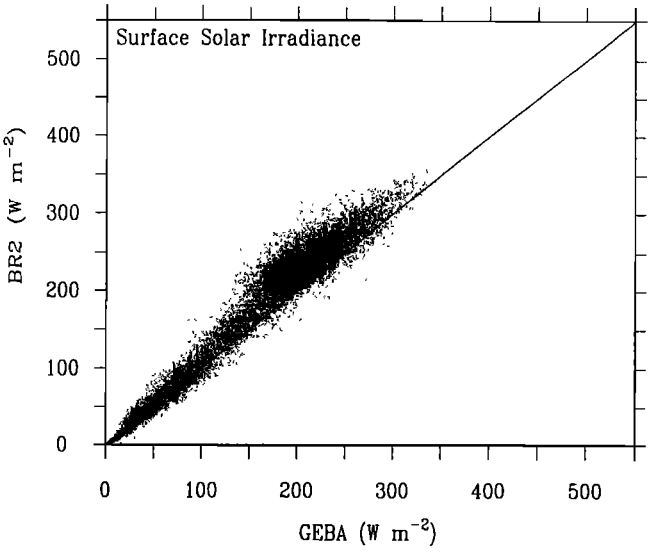

Figure 16. Surface solar irradiance from 21,000 monthly averaged surface observations from GEBA archives versus contemporaneous BR2 surface irradiance retrievals. Over 65% of the stations are between 30° and 60° north. The data are predominantly land-based. Oceanic examples are discussed in the text.

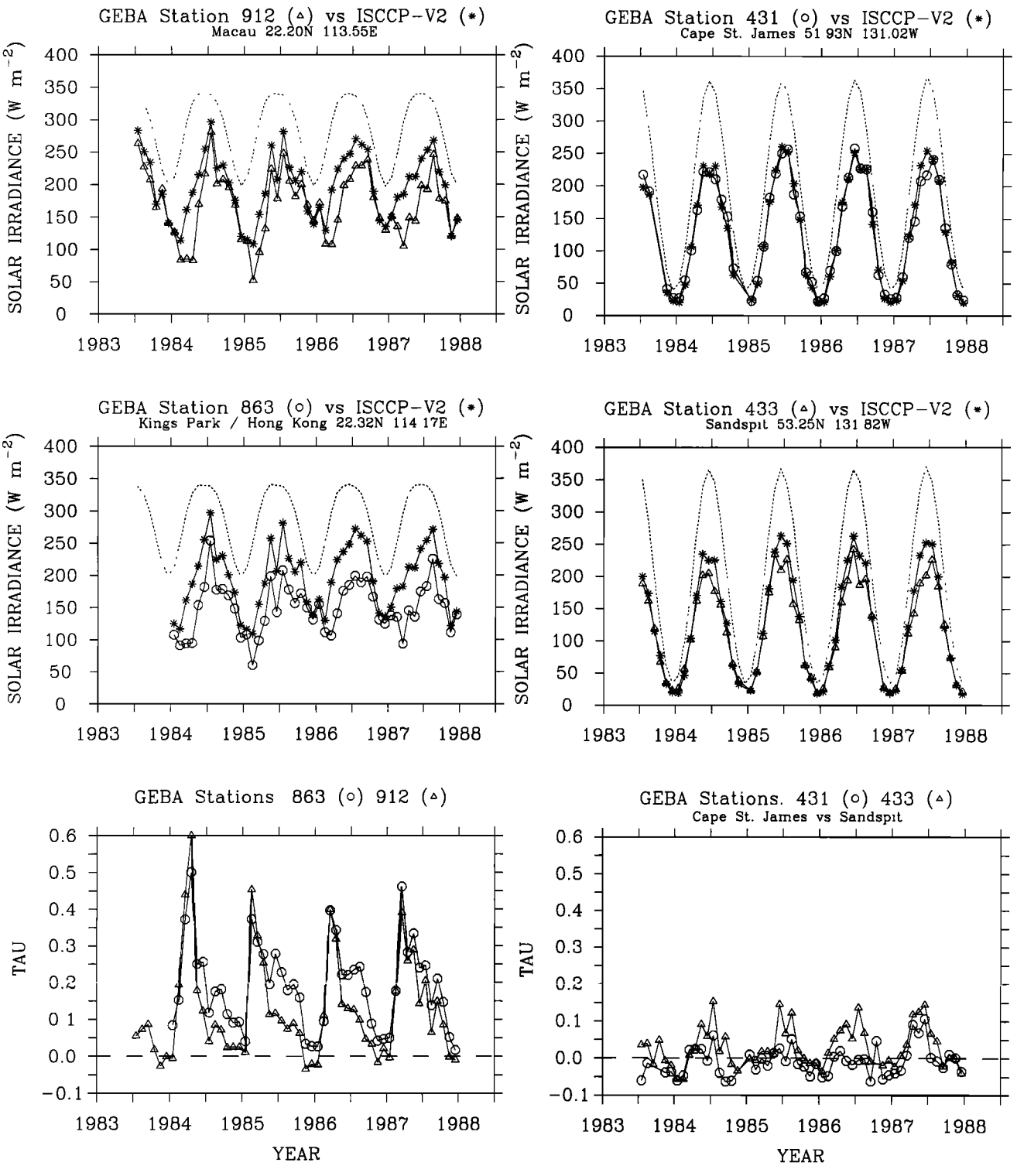

Figure 17. (Left (top and middle)) Comparison of the time series of monthly mean surface solar irradiance from BR2 (astersiks) and the measurements at Macau (triangles) , Hong Kong (circles). BR2 clear sky reference is shown by dashed curves; (bottom) equivalent optical extinction anomaly at Macau and Hong Kong. (Right) Like left panels but for Cape St. James and Sandspit, British Columbia.

do, however, show striking pattern consistency to the τ^* distributions retrieved at coastal locations.

The BR2 versus GEBA optical thickness anomaly (Plate 1) is generally higher over land than over ocean with broad highs in temperate latitude and tropical locations. Near zero values are found for most stations across Canada in North America and across the Eurasian continent at similar latitudes in all seasons. Of note is the band of τ^* ~0.12 across the former Soviet Union at 50°N, 30-135°E aligned with the route of the Trans-Siberian railroad in the spring (MAM) season (Plate 1). This pattern persists into the summer. Stations north and south have lower τ^* values. The τ^* values decreasing from > 0.3 near Hong Kong/Macau (22°N,134°E) to

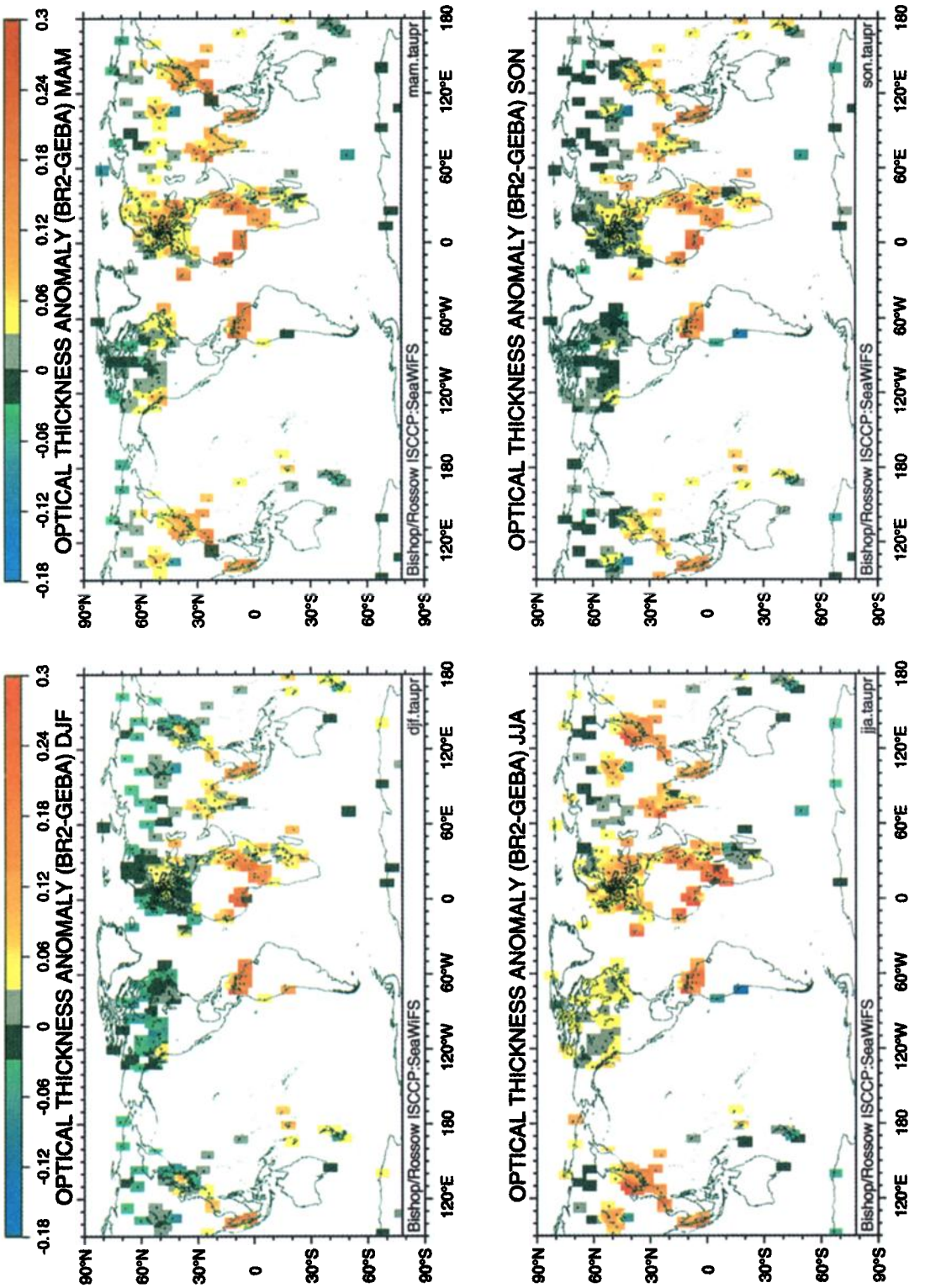

Plate 1. Global distributions of the optical extinction anomaly between the BR2 retrievals and the GEBA measurements of surface solar irradiance for December-January-February (DJF), March-April-May (MAM), June-July-August (JJA), and September- October-November (SON).

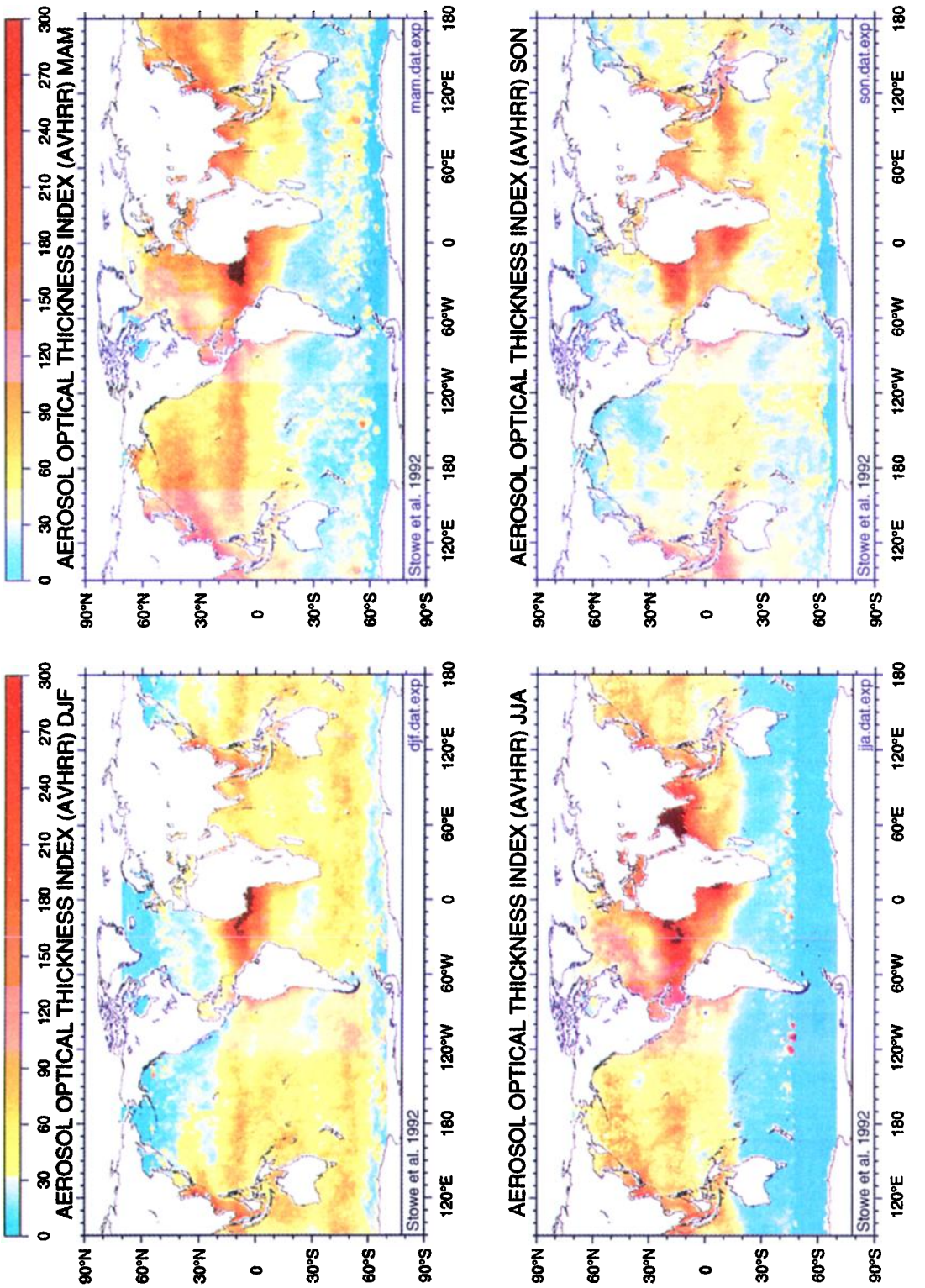

Plate 2. Global distributions of the index of aerosol optical thickness retrieved from AVHRR data for the same 4 seasons as depicted in Plate 1. The data are from *Stowe et al.* (1992).

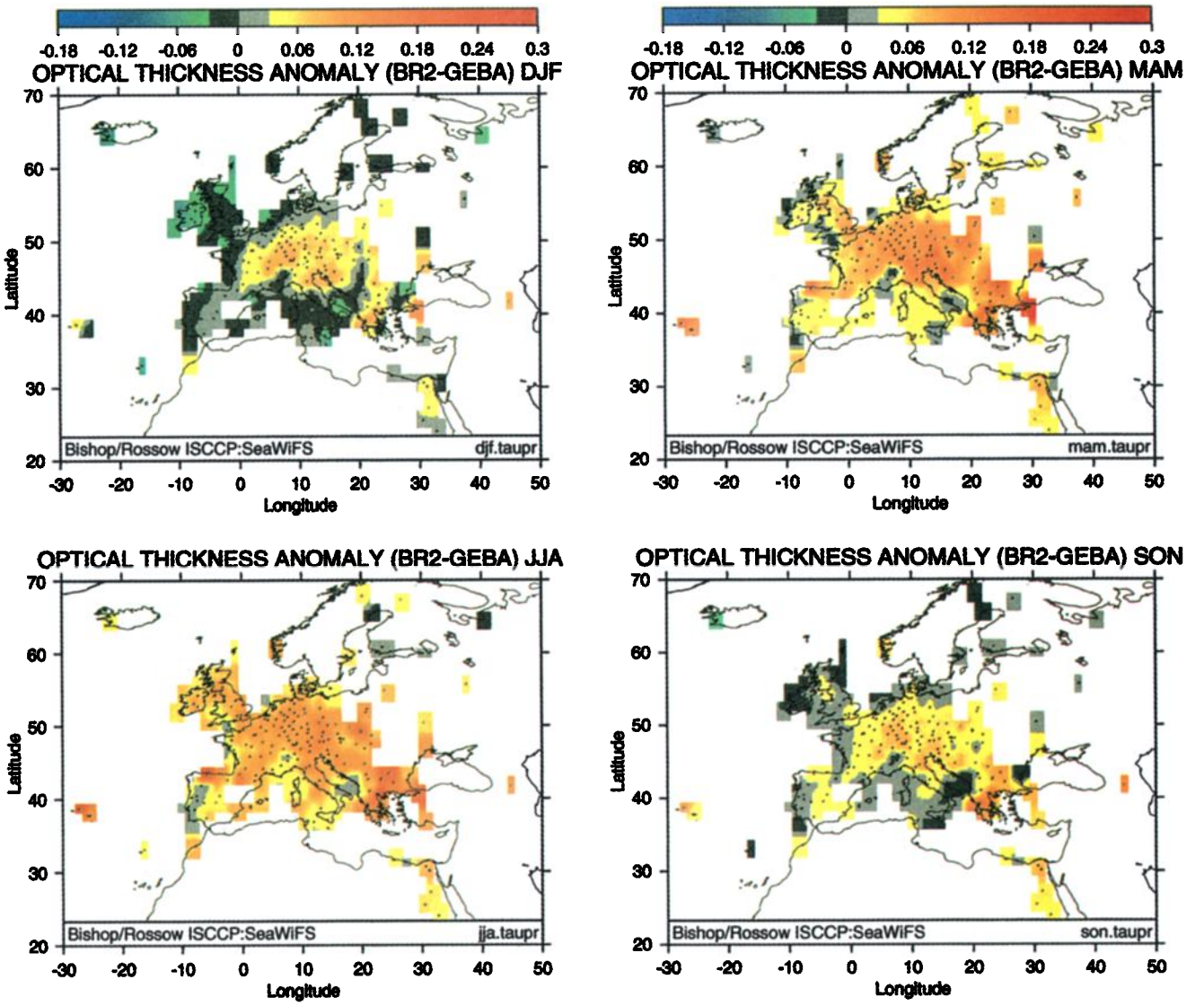

Plate 3. Like Plate 1, but for Europe.

~0.04 near Kwajalein (9°N, 168°E) in the springtime (MAM) are consistent with a decreasing influence of continentally derived mineral and anthropogenic aerosols moving from the coast into the ocean interior. Minimum anomaly is seen in the winter months (DJF) across this section. High values (τ^* ~0.2) are found generally in the tropics, especially in Africa and South America. High values occur seasonally in areas of the world where mineral dust aerosols of natural and anthropogenic origin are abundant. Biomass burning also is believed to contribute to the pattern. A general geographic pattern similarity is seen between the *Stowe et al.* [1992] aerosol optical thickness index for oceanic regions with our τ^* data for coastal and island regions (Plate 2). The seasonal variability of τ^* generally matches the modeled anthropogenic and natural mineral aerosol distribution results of *Tegen and Fung* [1994, 1995].

Plate 3 shows τ^* values at 1.25° resolution which depicts data for the north eastern Atlantic, Europe, Mediterranean Sea, and northern Africa which together contains most of the GEBA stations. The results for τ^* over land vary from lows of ~0.06 in winter and fall seasons to peak values around 0.2 in summer months. The overall optical extinction anomaly pattern for Europe matches well with inferred anthropogenic sulphate deposition and emission patterns [e.g., *Chadwick and Kuylenstierna*, 1990; *Langner and Rodhe* 1991]. For Europe in general, best agreement is seen for fall and winter, especially near the coasts. It is important to note that optical extinction anomaly values fall off near the coastlines in fall, winter, and spring to near-zero values suggesting that BR2 formulation is representative of background aerosol effects for calculating fluxes over northern hemisphere oceans in these seasons. The anomalous two data points on the Azores are unexplained and contrast with good agreement of island observations at Porto Santo to the southeast.

To summarize, the patterns seen in the BR2 versus GEBA comparison are exactly as expected due to the fact that atmospheric visibility was set at 25 km (equivalent aerosol extinction of 0.017) in our calculations. Secondly, aerosol indices such as the *Stowe et al.* [1992] product appear to be useful for improving our irradiance estimates over the ocean.

3.7. Comparison With Contemporaneous Oceanic Climatology

We compared BR2 irradiances for a variety of oceanic environments with the observations at selected GEBA stations (approximate latitudes, longitudes and station numbers in parentheses)

from all three major oceans and from both hemispheres. Results for Novazarevskaya (71°S, 12°E, 1457) and Mirnyy (67°S, 93°E, 1462), both located on the coast of Antarctica, show that BR2 data *underestimate* annual surface irradiance on the average by 4 and 5 W m^{-2}, respectively, At Mirnyy, the underestimate may be as much as 30 W m^{-2} in the austral spring. The underestimate (negative t*) is consistent with the aerosol loading of the southern polar atmosphere being much lower than our (BR2) assumed aerosol extinction parameterization of 0.014. It may also be caused by different cloud drop sizes and/or higher surface reflectivity in the real world compared to the retrieval schemes.

Further north at Invercargill, New Zealand (46°S, 168°E, 1150), and Port aux Francais, Kerguelen (49°S, 70°E, 1458) the annual mean bias is -3.4 and +9.9 W m^{-2}, respectively; monthly differences ranged from +17 to -4 and from +14 to -21 W m^{-2} at these two stations. The results at Invervargill, New Zealand are similar to those at Cape Grim, Australia (41°S, 145°E), which shows a 0 W m^{-2} annual bias over 8 years of data. The poorer performance of BR2 at Kerguelen illustrates the possible errors associated with the lack of geostationary satellite data with resulting incomplete characterization of the diurnal cycle of cloudiness over the Indian Ocean.

Results from two islands in the South Pacific, Nandi (18°S, 177°E, 1131), and Koumack, New Caledonia (21°S, 164°E, 1142), show BR2 to overestimate surface solar irradiance by approximately 8 W m^{-2}; these errors are equivalent to a 3% error in annual means for the two stations. Nevertheless, some months show as much as 30 W m^{-2} bias and require τ* values as high as 0.09 to bring the data together. Nearby at Samoa (14°S, 171°W, NOAA station), the BR2 data showed an annual average offset of +20 W m^{-2} from the NOAA surface observations. Kwajalein atoll (8°N, 168 E, NOAA stn) gives an annual bias of +10 W m^{-2}. Chichijima, an island station (27°N, 142°E, 893), in the Pacific, suggests data in error by as much as 60 W m^{-2} during the summer and an annual mean bias of +30 W m^{-2}. As discussed above, micrometeorological effects associated with large islands are likely to contribute to the large offsets at Samoa and Chichijima.

Surface irradiance at Atlantic Ocean locations, Porto Santo (33°N, 16°W, 195) and Sable Island (44°N, 12°E, 429), show similar behavior, but the BR2 data show annual biases of 0.5 and 1.6 W m^{-2}, respectively. Monthly differences range from +20 to -8 W m^{-2} at Sable Island (Figure 18) in a seasonal pattern high in the summer, low in the winter. As mentioned below this trend is also repeated in differences between BR2 data and ocean weather station climatology.

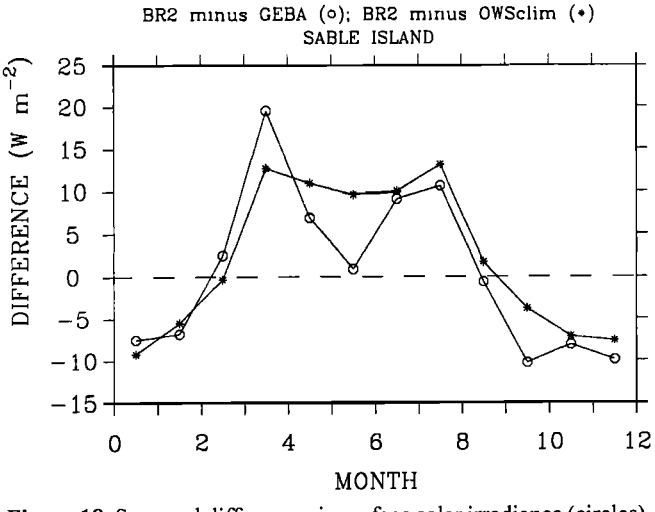

Figure 18. Seasonal differences in surface solar irradiance (circles) between BR2 and GEBA, and (astersiks) between BR2 and the climatology at Sable Island.

Micrometeorological and mesometeorological and local aerosol effects are also likely to explain the difference in irradiance data between open-ocean and coastal locations at middle to higher latitudes. This is illustrated in the comparison of three pairs of adjacent sites. Normoutier Island in the Atlantic (47°N, 2°W, 1253) has an annual bias of +0.4 W m^{-2} and a range of differences between +12 and -6 W m^{-2} over the year, while Bordeaux, France (45°N, 1°E, 1259), which has noticeably high aerosol loading, shows a +16 W m^{-2} annual bias and a summer time bias as high as 35 W m^{-2} (τ* as high as +0.09). Similarly, Lerwick in the Shetland Islands in the NE Atlantic (61°N, 10°W, 1276) and Valencia, Ireland (1335, 52°N), show +2.4 W m^{-2} and +6.2 W m^{-2} annual biases, the latter showing a monthly range +28 to -10 W m^{-2}.

3.8. Comparison With Ocean Weather Station Climatology

BR compared 5 months of calculated solar irradiance with the 1960's to early 1970's climatology from ocean weather stations (OWS) A, I, J, P and Sable Island [*Smith and Dobson*, 1984; *Dobson and Smith*, 1988]. In our present analysis the 8 year BR2 climatology is compared with the same ocean weather station data (Figure 19, Table 4). Differences are greatest in the North Atlantic in late spring At ocean weather station A, at 62°N, east of Greenland, BR2 data are higher than the climatology by 50 and 90 W m^{-2} for the months of May and June with an annual bias of +19 W m^{-2}. The corresponding values are +30, +45, and +9 W m^{-2} for Station I (at 59°N south of Iceland); +20, +10, and +5 W m^{-2} at Station J and +13, +11, and +2 W m^{-2} at Sable Island. The small bias in the annual means at the latter stations is due to compensating negative differences in the winter seasons. Data at OWS P in the North Pacific show a bias of +8 W m^{-2} in annual mean. The summertime +10 to +15 W m^{-2} bias at OWS P could be erased by assuming that NOAA 7 and not NOAA 9 radiances were correct (see, for example, Appendix Figure A2).

The data at OWS A, I, and from MLML, all in the vicinity of Greenland and Iceland, show interesting differences. Comparison of BR2 data and ocean buoy data from the MLML site, at almost the location of OWS I, indicates less than a 10 W m^{-2} bias (-4 W m^{-2} average) for the springtime months. This is much less than the difference at OWS I as discussed above. Because the ideal *a priori* setup of MLML for comparison with satellite observations (relative spatial homogeneity, contemporaneous high-frequency data) we assert that the MLML comparison gives an estimate of the error in the BR2 springtime irradiance for this region. The springtime differences found at stations A and I in the north Atlantic between the 1970s and our late 1980s climatology are significantly larger than uncertainties in our data and may be indicative of a physical change in the irradiance in this region. This change is not found at Sable Island (44°N) where the contemporaneous BR2 versus GEBA comparison and the BR2 versus the 1960s climatology (Figure 18) showed very similar patterns. The decreasing amplitude of difference between BR2 and OWS climatologies with latitude and the enhancement of differences in the North Atlantic versus the Pacific is consistent with patterns of shifts in climate between the two time periods compared [*Deser and Blackmon*, 1993; *Levitus et al.*, 1994].

3.9. Summary

The extensive comparison presented above shows that BR2 surface solar irradiances are in reasonable agreement with surface

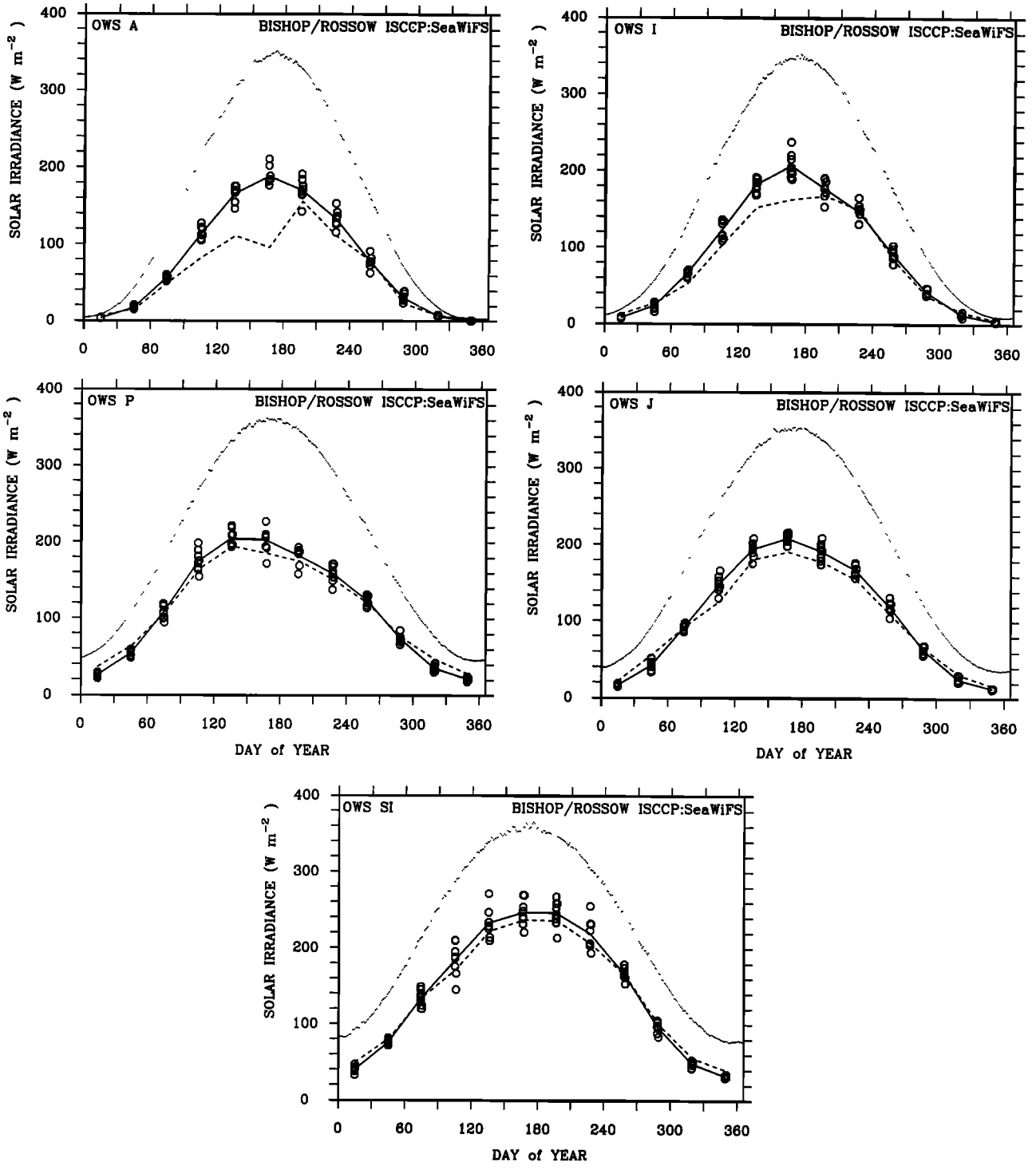

Figure 19. Comparison of surface solar irradiance from the late 1960s to the early 1970s climatology from ocean weather stations [*Smith and Dobson* 1984; *Dobson and Smith*, 1988] and BR2 (July 1983 to June 1991). Climatological data for OWS A (62°N 33°W), I (59°N 19°W), J (52.5°N 20°W), P (50°N 145°W) and Sable Island (44°N 60°W) are shown by dashed lines; mean annual cycle of the 8 years of BR2 data are shown by solid lines; individual BR2 months (circles); BR2 daily clear sky irradiance denote the upper envelope of the data.

observations, especially for oceanic regions. The comparison relied on observations of surface irradiance made during intensive field campaigns and/or long-term observations at climate monitoring sites. The ground data are of varying quantity and quality.

Comparison of the BR2 data at 280 km resolution with oceanic, local island, or coastal data (sections 3.2 and 3.3) shows the difficulty of interpreting the discrepancies between the two. Migrating weather systems and/or recurrent local meteorology are likely to affect the cloudiness at a single point and may be averaged out in the 280 km BR2 data. Our analysis suggests that the BR2 data are representative of the large-scale variations of solar irradiance at the surface.

We show that a source of error in the BR2 irradiance comes from the lack of geographic and temporal variations of aerosol

Table 4. Ocean Station Climatology Versus BR2 (1983-1991)

	OWS A (1961-1971)					OWS I (1957-1971)					OWS J (1958-1971)				
Month	Obs.	Int.	Pixel	s.d.	2-1	Obs.	Int.	Pixel	s.d.	2-1	Obs.	Int.	Pixel	s.d.	2.1
Jan.	6	3.2	3.9	0.4	-2.8	12	7.8	8.2	0.9	-4.2	21	15.9	13.4	1.7	-5.1
Feb.	15	16.9	18.6	2.5	1.9	27	23.3	24.0	4.7	-3.7	56	41.7	37.5	6.0	-14.3
March	49	56.1	59.5	4.5	7 1	53	66.2	67.0	4.1	13.2	92	91.4	87.0	5.2	-0.6
April	83	114.0	116.0	9.8	31.0	105	124.0	125.2	13.3	19.0	126	148.5	148.1	10.5	22.5
May	111	166.0	161.5	15.9	55.0	153	182.6	183.6	9.4	29.6	181	194.2	187.9	10.4	13.2
June	96	188.4	178.3	13.7	92.4	163	207.1	208.5	16.3	44.1	191	208.6	208.8	4.2	17.6
July	156	170.8	165.6	17.1	14.8	168	177.5	178.1	13.2	9.5	178	192.0	189.2	11.6	14.0
Aug.	111	133.7	131.9	13.1	22.7	150	147.6	149.0	11.0	-2.4	155	167.4	163.7	8.5	12.4
Sept.	78	77.7	79.6	8.2	-0.3	84	91.5	92.3	7.9	7.5	109	119.2	112.7	9.7	10.2
Oct.	23	30.4	32.8	6.0	7.4	37	42.6	43.5	4.1	5.6	65	63.1	58.4	4.3	-1.9
Nov.	8	7.8	9.2	0.7	-0.2	16	13.0	13.3	2.2	-3.0	31	24.6	21.2	3.4	-6.4
Dec.	2	1.3	1.8	0.2	-0.7	6	4.4	4.8	0.6	-1.6	16	13.0	11.3	0.9	-3.0
Average	61.5	80.5	79.9		19.0	81.2	90.6	91.4		9.4	101.8	106.6	103.3		4.8

OWS, ocean weather stations. All values in W m^{-2}. Obs., climatological (1970's) means for Stations A, I, J, and Sable Island from *Dobson and Smith* [1988]; for B and P from *Smith and Dobson* [1984]. Int., BR2 data interpolated to location of the station. Pixel, values of data from pixel containing the station; s.d., standard deviation of monthly irradiances over the 8 year time series.

extinction in the ISCCP and BR2 schemes. The error is larger over continents than over oceans and is largest in areas and seasons known to be polluted. Improvements to the retrieval algorithms cannot be implemented, however, until global information on aerosol distributions and aerosol optical properties become available. Here, we characterize the impact of aerosols on the BR2 surface irradiances with an equivalent optical extinction anomaly. Our comparison suggests that for open ocean areas far away from anthropogenic and mineral aerosol effects, the BR2 data are a reasonable representation of surface fluxes: τ^* is low, and the bias in the BR2 rarely exceeds +10 W m^{-2} in the annual mean. At high-latitude coastal locations, there is a general tendency to overestimate fluxes in summer conditions and underestimate in the winter, again perhaps due to the seasonality of aerosols or of cloud optical properties (e.g., ice cloud particle size) not properly parameterized; however, the disagreement seldom exceeds 20 W m^{-2} in the monthly means.

The BR2 data show biases, generally positive in the summer and negative in the winter, when compared with island and weather station data. Since there is no absolute calibration in place for the satellite radiances, we could reduce most of the summertime positive bias in the data by assuming NOAA 7 radiances are correct (Appendix A1) and adjusting the NOAA 9 and NOAA 11 radiances accordingly. There is a 7 to 10% uncertainty in the ISCCP radiance calibrations. Two arguments suggest that errors are certainly less than the 15% suggested by *Frouin et al.* [1995] (section 3.4). The first comes from the analysis of indirect and direct calibration evidence [*Brest et al.*, 1997] which shows that ISCCP calibrations fall in the "middle" of possible results. The second is that a +15% adjustment makes the MLML data disagree more. (Table 4). While we disagree with the *Frouin et al.* [1995] suggested adjustment of radiances, the C1 versus CX comparisons at Wisconsin (section 3.1) suggest that there may be a nonlinear effect on retrieval of surface irradiance using the average cloud properties of C1 compared to retrieving irradiances directly from the ~80 CX pixels and then averaging the results. Thus the upward radiance adjustment suggested by *Frouin et al.* [1985] may, in fact, be the magnitude of the correction needed to compensate for this bias. We

Table 4. (continued)

	OWS P (1959-1975)					Sable Island (1969-1980)				
Month	Obs.	Int.	Pixel	s.d.	2-1	Obs.	Int.	Pixel	s.d.	2-1
Jan.	26.6	25.4	22.0	2.6	-1.2	49	39.8	36.9	3.8	-9.2
Feb.	52.7	54.2	50.8	5.1	1.5	81	75.5	71.7	3.6	-5.5
March	94.7	107.3	105.6	10.3	12.6	134	133.7	126.9	11.7	-0.3
April	151.7	174.9	172.2	11.4	23.2	172	184.7	180.2	21.5	12.7
May	186.0	204.7	205.2	10.8	18.7	222	232.9	228.3	21.4	10.9
June	187.2	202.0	201.0	17.1	14.8	237	246.6	241.9	17.9	9.6
July	172.9	182.3	185.9	10.1	9.4	236	246.0	246.5	16.4	10.0
Aug.	146.9	159.0	158.7	12.0	12.1	206	219.1	217.8	20.9	13.1
Sept.	114.3	124.1	120.6	6.4	9.8	165	166.7	165.6	9.0	1.7
Oct.	73.7	73.8	70.6	5.2	0.1	101	97.2	96.8	9.6	-3.8
Nov.	36.7	35.3	32.5	4.4	-1.4	56	48.9	48.2	4.4	-7.1
Dec.	23.2	22.0	18.6	2.1	-1.2	40	32.4	30.0	2.7	-7.6
Average	105.5	113.8	112.0		8.3	141.6	143.6	140.9		2.0

note, however, that such a bias may be determined by the relative scales of cloud systems sampled versus the area represented by the C1 pixel. Irrespective of satellite radiance calibration adjustment, the negative winter biases will remain about the same magnitude and require some other explanation.

Negative wintertime biases remain at some locations even after eliminating aerosol effects since τ^* values required to bring some data in line are unrealistically low (-0.07) when the existing background aerosol extinction coefficient is only 0.014. This points to other causes of the discrepancies. Errors could arise from incomplete parameterization of reflections at high solar zenith angles from the sides of clouds in broken conditions, or from the assumption of constant average cloud liquid drop size (10 μm), or from lack of inclusion of the radiative properties of ice clouds. It is possible that there may not be a bias at all but that the problem may lie in our reliance on coastal/island stations which experience different cloud properties than the surrounding 280 km ocean area. In any case, the biases on monthly timescales are small, <10 to 20 W m^{-2}.

4. Variability of Solar Irradiance 1983-1991

In this section, we present an analysis of the variability of solar irradiance for the period 1983-1991. The validation analysis above suggests that while some biases may exist in the BR2 data set, the biases are small over oceans and do not appear to vary greatly from year to year.

We have averaged our data zonally at 2.5° globally, and for the Atlantic, Pacific, and Indian Ocean basins, to examine the interannual variability on a seasonal basis over the entire 8 year time series. After averaging, the mean for each month at a particular latitude is subtracted from the 8 year average for the same month to produce an irradiance anomaly time series.

4.1. Zonal Mean Anomalies for Oceans and Seas

Plate 4 shows the latitudinal and temporal variability of monthly mean BR2 surface irradiances zonally averaged for the ocean. Most interannual variability is within +5 and -5 W m^{-2} of the monthly mean. Strongest anomalies occur in the polar regions where interannual differences may exceed +25 and -30 W m^{-2}. Strong negative anomalies occurred during June and July 1989 and 1990 in the northern hemisphere and during January 1986 in the south. Intense positive anomalies are seen over the Arctic Ocean for June and July 1987, 1988, and 1985. Interestingly, the southern hemisphere circumpolar current region at 60°S, one of the cloudiest on Earth, is next in our ranking of global interannual variability. The strongest positive anomaly year was 1984/1985; the most intense negative anomalies were in 1985/1986 and 1989/1990. In the tropics, most values scatter between +10 and -10 W m^{-2}.

A band of -5 to -10 W m^{-2} anomaly is seen to extend from pole to pole for the months November and December 1988 through mid-1989. This period corresponds to the only strong La Nina within the entire record. Because this anomaly began with the November 1988 NOAA 9 to NOAA 11 satellite transition, its magnitude and, indeed its reality remain to be verified. Overall, the data suggest consistency across the entire time series of +10 to -10 W m^{-2}.

The irradiance anomaly patterns for globally averaged data show similar patterns but with reduced amplitudes. The ocean intensification is explained by the fact that oceans are more cloudy than continents (see, for example, *Bishop and Rossow*, [1991]).

4.2. Zonal Mean Anomalies for the Pacific Ocean

The Pacific Ocean is strongly influenced by El Nino - Southern Oscillation (ENSO) phenomena. The zonal anomaly time series in the tropics reflects this fact (Plate 4). The strong 1982/1983 El Nino preceded the start of the ISCCP data set. 1984 stands out as a +20 to 25 W m^{-2} anomaly in the tropics. The 1986/1987 El Nino resulted in an overall decline in irradiance of as much as 30 W m^{-2} averaged over the entire tropical Pacific. Near 45°N, 10 to 25 W m^{-2} negative anomalies occur during the summers of 1983, 1987, and 1988 and a 10 to 20 W m^{-2} positive anomaly in 1991. The "La Nina" band remains a feature of the time series but is reduced in magnitude compared with the all-ocean averages. The intense anomalies at the polar extremes of the figure are consistent with earlier described patterns but may be enhanced because of numerically few points contributing to the averages.

4.3. Differences Between the Atlantic and the Pacific

Bishop and Rossow [1991] noted that the Atlantic Ocean received much greater surface solar irradiance, especially in the northern hemisphere. Here, we have computed a zonally averaged difference of surface irradiance between monthly zonal means from the Atlantic and Pacific Oceans (Plate 5). Consistent with BR, we find that summer time surface solar irradiance at 45°N over the Atlantic is typically greater than 50 W m^{-2} higher than that of the Pacific Ocean. This band of positive anomaly extends as far south as 10°N. A weaker positive anomaly pattern is found in the Southern Ocean from 5°S to approximately 40°S. In this zone the two oceans tend to oscillate positively and negatively relative to one another on a seasonal basis. In the equatorial band, 5°N to 5°S, patterns of difference indicate that the Atlantic typically receives as much as 25 W m^{-2} less than the Pacific except during El Nino years. Positive anomalies exceeding 50 W m^{-2} are also found in the Southern Ocean in a band centered on 60°S. The Atlantic versus Pacific anomalies are significant in terms of both the surface heat budget and the driving force for marine productivity. The 60°S band is particularly important since it occurs over the ocean regions where dissolved nutrient concentrations do not limit marine photosynthesis. *Bishop and Rossow* [1991] have already noted that seasonal deficits of surface ocean pCO_2 and the occurrence of phytoplankton biomass are more intense in the South Atlantic compared to the South Pacific. Thus we see that the differences between the two oceans are consistent seasonally on a year-to-year basis with interruptions due to ENSO fluctuations.

5. Conclusion

In this study, we present a new data set of daily solar irradiance at the surface for July 1983 to June 1991, resolved at 2.5° latitude by 2.5° longitude for the globe. The long time series is derived from the cloud radiative properties retrieved by ISCCP from radiances measured by four geostationary and two polar orbiting weather satellites. A new version of our fast computational scheme calculates the average and temporal fluctuations of surface solar irradiance (and PAR) on timescales relevant to marine phytoplankton physiology using ISCCP cloud data.

The data set has been compared with those from a wide range of ocean mooring, island locations, and GEBA. In open-ocean, clean-air locations the comparison was good when the effects of weather systems are averaged out. The comparison was not and should not be so successful at large islands or coastal stations

where local orographic and other meteorological effects create systematic differences between the station and surrounding waters.

Errors in our retrievals are likely to come from many sources. One factor we have identified is the spatially and temporally varying aerosol loading in the atmosphere: At continental sites the difference between the satellite retrievals and the surface observations were largest in known polluted regions and in known mineral dust aerosol areas. This error can be corrected once we have an improved distribution of aerosol loadings and their radiative properties. Another source of error may be satellite calibration. We have used ISCCP-calibrated radiances in our retrievals. While we cannot rule out other calibration issues, a further global adjustment of the ISCCP C1 radiances improved the comparison at some locations and degraded the comparison at other ground stations. No reasonable correction could be made to bring surface observations and retrieved data from either Bermuda or Samoa into exact agreement. Remaining sources of error may stem from the ancillary data (e.g., TOVS ozone and water vapor) used in the ISCCP retrieval and from the assumptions and physics employed in the ISCCP retrieval algorithms employed (e.g., uniform cloud drop size distribution, no distinction between water and ice clouds). These would translate directly into changing values of cloud fraction and cloud optical thickness, the starting point of the BR2 algorithm. Evaluation of the ISCCP algorithm is beyond the scope of the present study. However, as ISCCP products are continually evaluated by the wide user community, quantitative estimates of this error may be possible when improved ISCCP algorithms are implemented for the next generation product.

Our analysis shows that surface observations from large islands with their own micrometeorology may show a systematic bias versus the mean irradiance from a large (280 km) area. Observing locations with eastward or poleward ocean exposures appear to be undesirable for validating ocean fluxes due to such effects. We also conclude that ocean buoys should be further evaluated as platforms for "surface truthing" satellite data, especially in conjunction with carefully chosen island sites. Buoy-mounted sensors are not perfected since they lack the stability and ease of access of land sites. The TOGA-TAO array of moored buoys [*Hayes et al.*, 1993] which currently spans the tropical Pacific appear to be attractive platforms for resolving issues of tropical surface solar irradiance differences. Data collection began at several equatorial locations beginning late 1991, too late for comparison with the existing time series described above.

During the course of our analysis, errors were found, and subsequently corrected, in significant percentage of the high-frequency surface observations examined. These errors were found by comparing the clear sky irradiance envelope of surface data with that calculated in our model and examining instrument calibration histories. The identified errors were corrected and have no further impact on the analysis presented here. However, similar problems may contaminate GEBA data sets as well. Since they are monthly averages, errors of this magnitude are nearly impossible to detect. Thus ground observation programs do not but must have sufficient resources for expanded data collection and for adequate quality control. Arrays of sensors, such as deployed during the 17 day FIRE/SRB experiment, compatible with the spatial scale of satellite observations are most desirable. Surface observations have not been but must be analyzed in terms of hourly or shorter variability since monthly averages are not sufficient to separate cloud and aerosol effects.

At the present time, international efforts are under way to establish a high-quality array of observing sites as part of the WMO/WCRP Baseline Surface Radiation Network (BSRN) [*World Climate Research Program*, 1991]. These sites now observe strict protocols to ensure data quality and long-term validity to the observations and will continue to play a critical role in validation of retrievals of surface solar irradiance. Needed, however, are more BSRN sites at coastal locations that are facing equatorward with little landmass to the west.

The phased obsolescence of satellites and their replacement by successive generations presents a scientific challenge to the use of the data to examine changes in irradiance through time. Consistent with *Bishop and Rossow* [1991], we find significant regional and temporal variability in the surface irradiance. Over most of the oceans the systematics of the variability is consistent with that known from other climate parameters, suggesting that the data set may be useful for analysis of interannual variability. A new feature is the large variability in insolation over the southern Atlantic and Pacific Oceans.

As a result of the validation effort presented here, we have implemented a revised scheme for SeaWiFS for 280 and 30 km data, and the scheme is being used in the production of a 0.5° by 0.5° product for SeaWiFS using ISCCP DX data.

Appendix

The revisions to the Bishop and Rossow scheme and input data sets (and the resulting 8 year time series data produced) include data adjustments due to changes in NOAA satellite radiance calibrations (section A1); a scheme to trap and replace unexpected bad data (section A2); an improved scheme to fill missing data (section A3); and modifications to the BR scheme (section A4). These steps were necessary to implement production of global surface solar irradiance fields on 3 hour time steps as required by SeaWiFS. We also describe the availability of data (section A5).

A1. Adjustments to Data Due to Satellite Sensor Calibration Changes

Data from the advanced very high resolution radiometer (AVHRR) instruments carried aboard the NOAA polar orbiting spacecraft are used to normalize radiance data from all geostationary satellites contributing to ISCCP. Offsets in radiance calibrations from NOAA 7, 9, and 11 used in ISCCP cloud retrievals became apparent in empirical orthogonal function (EOF) analyses of a 7 year (1983-1990) time series computed using the *Bishop and Rossow* [1991] scheme [*Rossow and Cairns* 1995; see also *Klein and Hartmann* 1993]. To correct these offsets, ISCCP C1 radiances were multiplied by 0.945 for data spanning July 1983 to January 1985 (NOAA 7), unaltered for February 1985 to October 1988 (NOAA 9) and multiplied by 1.119 for November 1988 to June 1991. The midperiod calibrations were assumed to be correct because of excellent agreement of satellite-retrieved solar irradiances and surface observations during the First ISCCP Regional Experiment/ Surface Radiation Budget (FIRE/SRB) experiment [*Whitlock et al.*, 1990]. ISCCP has a scheme to track sensor drift within the three periods, and so secondary drift correction was unnecessary. The adjusted radiances are then used to obtain revised cloud optical thickness values from the C1 lookup tables. (ISCCP has incorporated similar adjustments directly into the new DX, D1, and D2 products). Surface irradiance in cloud-free regions was minimally affected because clear-sky radiances are computed using the *Frouin et al.* [1989] formula. After correction, NOAA satellite transitions were undetectable by EOF analysis of the data.

A2. Bad But Not Missing Data

Animations of daily clear sky irradiance fields showed unexpected variability in regions near high topography. This was traced to unexpected bad Tiros Operational Vertical Sounder (TOVS)

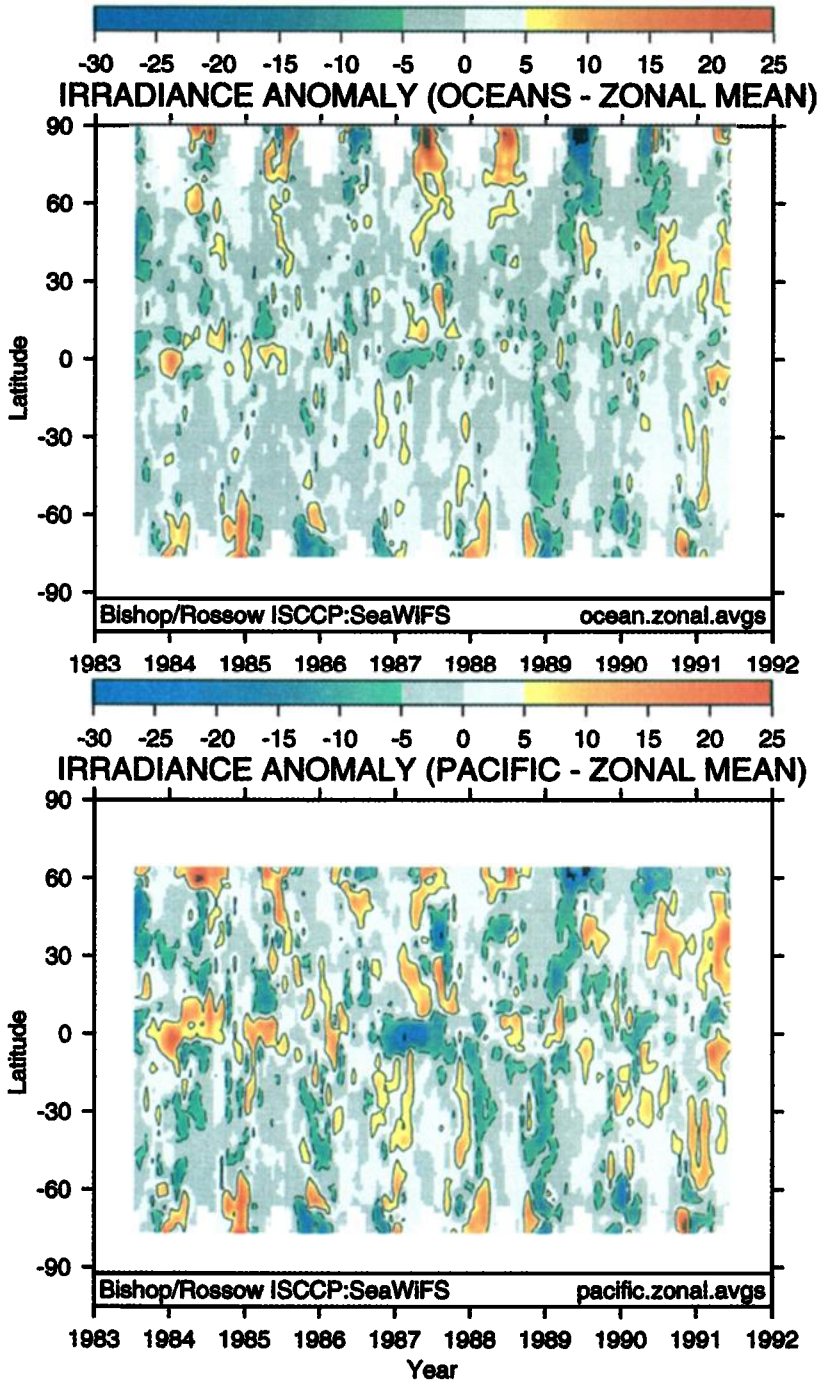

Plate 4. Latitude - month distribution of the seasonal departure in the zonally averaged surface solar irradiance from mean monthly irradiance for July 1983 to June 1991. (top) for oceans and seas. (bottom) for the Pacific ocean. El Nino Southern Oscillation effects are readily seen in the Pacific Ocean anomaly time series in the tropics.

(surface pressure, ozone, precipitable water) data in the ISCCP C1 product. Bad values were trapped by referring TOVS surface pressure to the monthly climatology of surface pressure [*Oort*, 1983]. To fix the problem, ozone, water, and surface pressure arrays were initialized with climatological values, and bad data were replaced with the climatological value or the last encountered good ISCCP value at that location.

A3. Input Data Filling Schemes

One or more of the eight 3-hour time intervals sampled by ISCCP per 24 hour day can lack cloud optical thickness values or have no data (both cloud fraction and cloud optical properties are missing). The former occurs when the solar zenith angle exceeds 78.5° (but less than 90°) and hence "day" is defined as "night" by ISCCP because of the difficulty of cloud optical property retrievals. Thus dawn, dusk, and some polar data sets require cloud optical properties to be filled. A total loss of cloud data occurs in the polar regions when there are frequently no valid data for a 3 hour time interval due to the lack of geostationary satellite coverage. The approach adopted in this case for solar zenith angles less than 90° was to first fill the cloud fraction value and then to assign a corresponding cloud optical thickness.

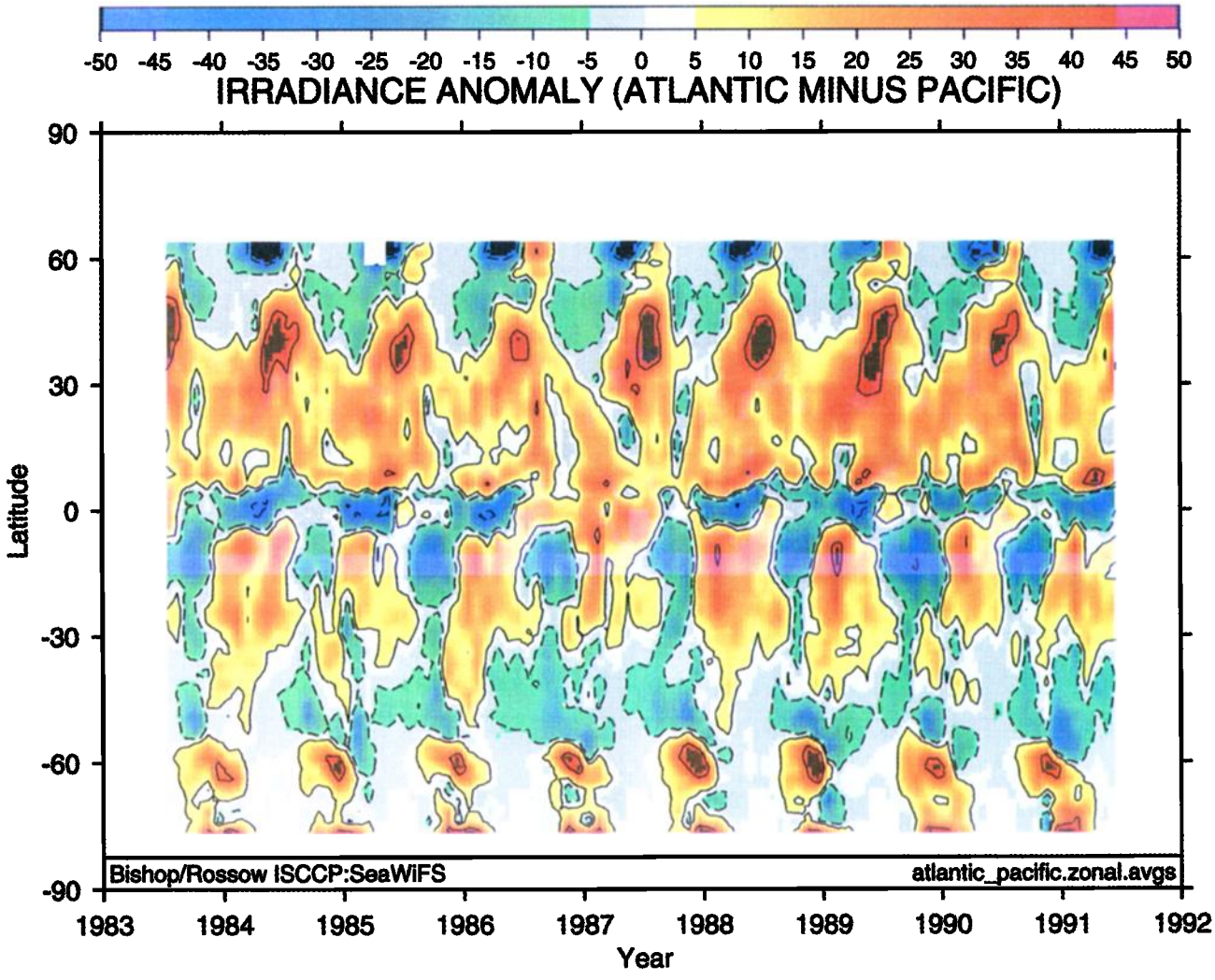

Plate 5. Latitude - month distribution for difference in solar irradiance Atlantic minus Pacific for July 1983 to June 1991.

Missing cloud fraction data were filled with a progressive scheme as follows: (1) zonal (at 5° resolution) averaged cloud fraction arrays were constructed and filled by interpolation for five surface-type categories corresponding to land, Atlantic, Pacific, and Indian oceans, and seas (including the Arctic Ocean); (2) a "day light" time-averaged 2.5°x2.5° cloud fraction array was computed from valid "day light" cloud fraction data; "day light" in ISCCP data is defined by solar zenith angle less than 78.5°; (3) a 24 hour averaged 2.5°x2.5° cloud fraction array was constructed and filled by interpolation with the following precedence: (1) from neighboring points (+/- one pixel E/W) in longitude; (2) from neighboring points (+/- one pixel N/S) in latitude; (3) from averaged daily data from the previous day at the same location; and (4) from surface type-specific zonal means for that day (from zonal cloud fraction). Finally, for each 3 hour ISCCP time step, missing data in each cloud fraction array were filled from the day time average cloud fraction array if any day time data are present, or from the 24-hour-averaged filled cloud fraction array. Thus all eight cloud fraction arrays are filled with data in a hierarchical fashion designed to preserve most of the diurnal variability of cloudiness.

Missing cloud optical thickness data occur in cases where no cloud retrievals were performed due to missing data, or in cases of daylight and solar zenith angle >78.5°. In these cases, each 3 hour cloud optical thickness field was filled using the surface type-specific zonal means of cloud optical thickness binned as a function of cloud fraction and the corresponding cloud fraction value from the filled 3 hour array.

Surface reflectance over the ocean was set to 0.06 as was done in the version 1 [*Bishop and Rossow*, 1991] production. This was necessary to trap high ISCCP C1 surface reflectance values due to Sun glint. The effectiveness of all of the above improvements was judged by animation of cloud property fields and spatial EOF analysis.

A4. Revised Bishop and Rossow Algorithm

Although the *Bishop and Rossow* [1991] model has undergone revisions, the fundamental approach has remained the same. Since all input data fields for each 3 hour ISCCP time step (surface pressure, ozone, precipitable water, surface reflectance, cloud fraction, and cloud optical thickness) are filled prior to performing the solar irradiance computations, the need for a "daily sampling correction factor" as described by *Bishop and Rossow* [1991] has been eliminated.

Algorithm. The algorithm for surface solar irradiance (referred to herein as BR2) utilizes the following ISCCP data: solar zenith

angle (μ_o), atmospheric water vapor profile (H_2O) and ozone column abundance (O_3), cloud fraction (CF), cloud optical thickness (τ), visible surface reflectance (R_S), surface type (land, water, coast, ice), and surface pressure (P_S). The major algorithm components are described by equations (A1)–(A5).

First, the clear sky component of solar irradiance is computed:

$$Q_{CLR} = (1\text{-}CF)\, f(S_o, d, \mu_o^*, O_3, H_2O, R_S, Vis, P_S) \text{ W m}^{-2} \quad (A1)$$

$$Q^*_{CLR} = f(S_o, d, \mu_o^*, O_3, H_2O, R_S, Vis, P_S) \text{ W m}^{-2} \quad (A2)$$

$$Q^{*C1}_{CLR} = f(S_o, d, \mu_o^*, O_3, H_2O, R_S, Vis, P_S) \text{ W m}^{-2} \quad (A3)$$

Q_{CLR} is the solar irradiance at the surface under clear sky conditions derived using the formula, f, of *Frouin et al.* [1989] and the completely filled input data sets. Q^*_{CLR} is Q_{CLR} assuming a cloud fraction of zero. Q^{*C1}_{CLR} is also evaluated with CF of zero whenever the 3 hourly data are unfilled. The *Frouin et al.* [1989] formula includes specific parameterization of the effects of variable surface reflectance, water vapor, ozone, aerosols, and surface pressure. The solar flux to the top of the atmosphere (S_o) is 1367 W m^{-2}. Corrections for seasonal variation in Sun-Earth distance (d) are included. The solar zenith angle (μ_o) averaged over the 3-hour period containing the ISCCP observation is denoted μ_o^*. Surface reflectance, R_S, is held constant at 0.06 over the ocean and set to the ISCCP (geographically and temporally varying) value over ice and land. This was done because Sun glint contributes to oceanic values reported in ISCCP data. The use of surface reflectance values in place of albedo is probably an underestimate for vegetated surfaces, close to truth for deserts, and an overestimate for ice and snow-covered surfaces. Visibility (Vis) was assumed constant at 25 km (but could be varied) and is the parameterization of aerosol effects. A 25 km visibility is equivalent to an atmospheric extinction coefficient of 0.014. We will evaluate the validity of this assumption in a later section.

Next we treat the cloudy sky component of irradiance:

$$Q_{CLD} = CF\, Q_{DIR}\, (1 - A_Z)\, (1 + A_S R_S + (A_S R_S)^2) \text{ W m}^{-2} \quad (A4)$$

The cloudy sky component of the calculation (Q_{CLD}; equation (3)) begins with the direct solar flux to the cloud top (Q_{DIR}) which is Q_{CLR} evaluated with zero surface reflectance and zero cloud fraction. A fraction of that flux is reflected back to space using a solar zenith angle dependent cloud albedo, $A_Z(\tau, \mu_o^*)$. The remaining transmitted fraction exiting the cloud base, not absorbed by the surface (determined by surface reflectance, R_S), is reflected upward and is reflected downward again from the cloud base (determined by spherical cloud albedo, $A_S(\tau)$). The term, $(A_S R_S)^2$, new to the BR algorithm, adds the effects of a second ground to cloud to ground path and is important only over cloud-covered high albedo surfaces.

The spherical (A_S) and directional (A_Z) albedos are related to the ISCCP optical thickness values at 0.6 μm. Although these albedos vary somewhat with wavelength over the whole solar band because of varying absorption by water, we can neglect this variation for two reasons. First, significant changes in the albedo occur only at wavelengths larger than 1.5 μm where there is much less solar radiation and much more absorption by water vapor. Thus these wavelengths contribute little to the total radiation at the surface. Second, in the presence of clouds, radiation at these longer wavelengths is absorbed by the cloud rather than by the water vapor; however, the difference in cloudy and clear surface irradiance is still very small [cf. *Rossow and Zhang*, 1995]. Although we present our calculations of total solar irradiance in this paper, our objective for SeaWiFS is to deduce the variability of PAR [400-700 nm irradiance], for which this representation of the cloud albedos is nearly exact. There are almost no long-term surface observations for PAR.

Rather than being computed in real time, A_S and A_Z are derived from cloud optical thickness using lookup tables. These tables are obtained from full Mie calculations and provide the key physical link between the observed cloudy scene reflectance and the total cloud transmission which lies at the heart of all methods for calculating surface solar irradiances [e.g., *Tarpley*, 1979; *Gautier et al.*, 1980; *Darnell et al.*, 1988]. Use of lookup tables gives the BR2 scheme a major improvement in speed while retaining most of the scattering physics.

The computation of total incident solar irradiance (Q_{TOT}) is the sum of clear (Q_{CLR}) and cloudy sky (Q_{CLD}) components (calculated every three hours).

$$Q_{TOT} = \Sigma(Q_{CLR} + Q_{CLD}) \text{ W m}^{-2} \quad (A5)$$

$$R = \Sigma Q^{*C1}_{CLR} / \Sigma Q^*_{CLR} \quad (A6)$$

A data quality indicator, R, is the ratio of the daily sums of 3 hourly irradiance computed only when ISCCP C1 data are present (equation (A3)) to the sums for all 3 hour time periods (equation (A2)). For most of the globe the R ratio is close to unity (all eight ISCCP observations are present) because of extensive daily coverage by multiple geostationary and polar orbiting satellites which contribute data to ISCCP.

A5. Availability of Data.

The 8 year (July 1983 to June 1991) time series of surface solar irradiance is available by request or via the network from the Archives at the National Center for Atmospheric Research (NCAR), Boulder, Colorado. The NCAR data set reference is "DS741.0 SURFACE SOLAR IRRADIANCE BY BISHOP." Data fields include daily clear sky irradiance (Q^*_{CLR}), daily and monthly averages of irradiance including the effects of clouds (Q_{TOT}), daily data quality ratio (R), and the standard deviations of daily Q_{TOT}. Details of data access may be obtained from the authors

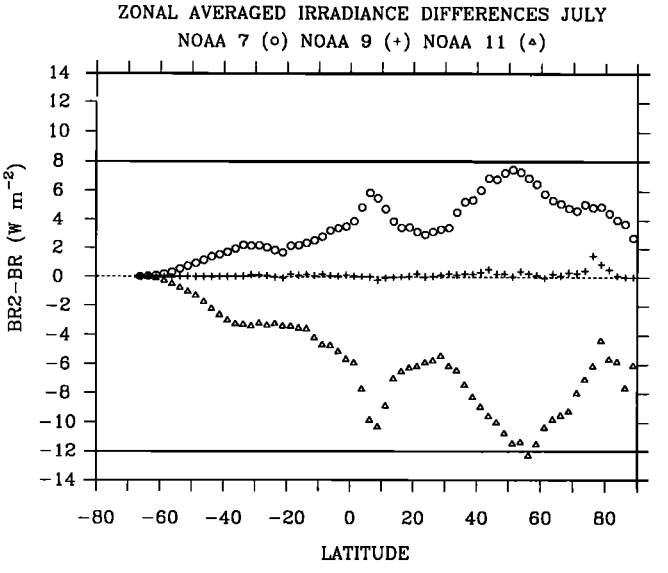

Figure A1. Latitudinal profiles of the difference in July surface solar irradiance between the BR2 and BR algorithms for data from NOAA-7 (circles), NOAA-9 (pluses) and NOAA-11 (triangles).

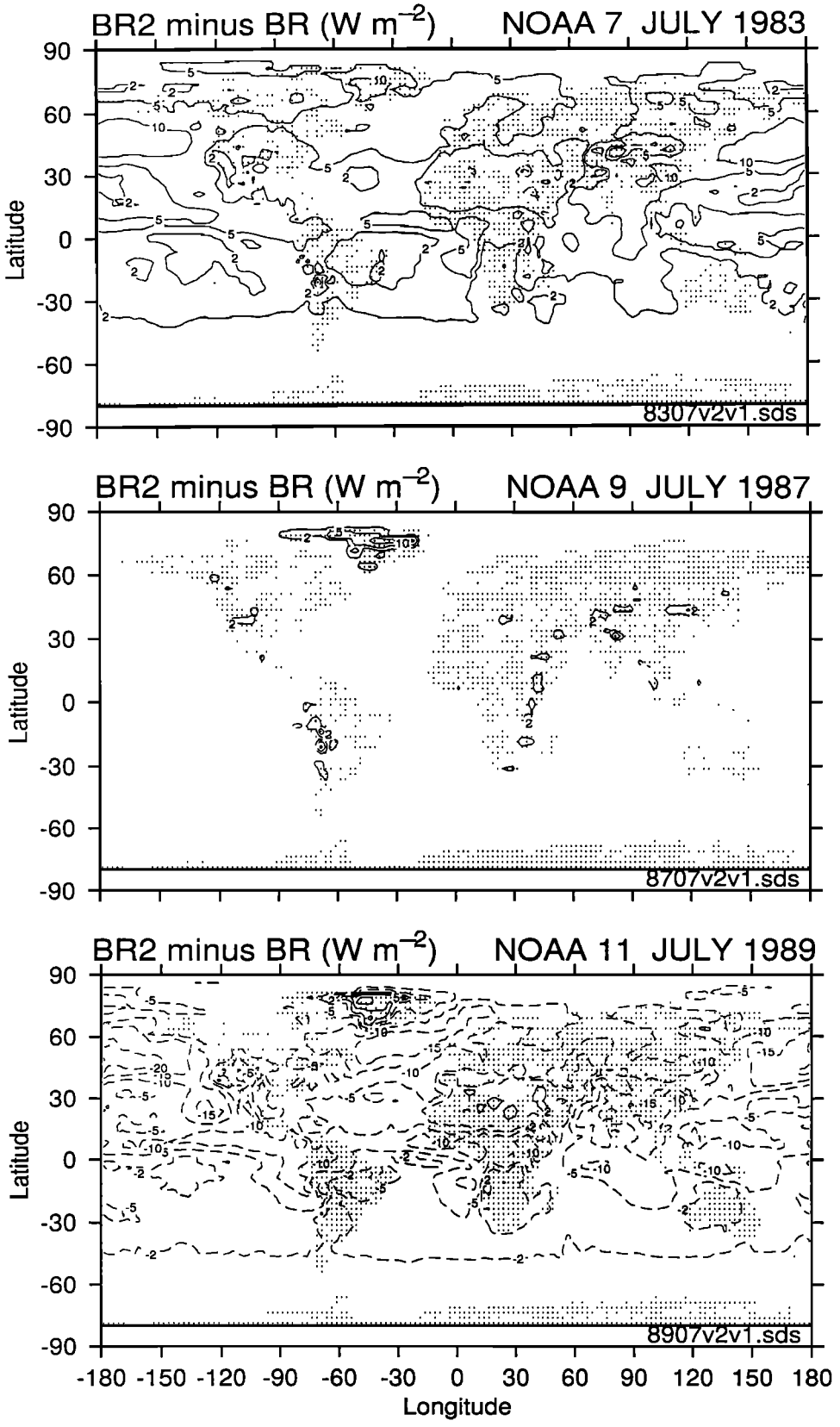

Figure A2. Differences (BR2 minus BR) July 1983, July 1987, and July 1989 illustrating the effects of adjustment of radiance calibrations for (top) NOAA 7, (middle) NOAA 9, and (bottom) NOAA (11) time periods.

or from NCAR. This data set is our production version 1.9 but for simplicity will be called BR2 in the discussion this paper.

A6. Differences

Differences between the original *Bishop and Rossow [1991]* data and those for the revised scheme were analyzed for July 1993 (NOAA 7), July 1987 (NOAA 9), and July 1989 (NOAA 11). On a zonally averaged basis, differences (BR2 - BR) for July 1983 and 1989 show a maximum of + 8 W m^{-2} and minimum of -12 W m^{-2} at 60°N, respectively (Figure A1). Minimal changes were noted for July 1987. In a spatial analysis (Figures A2) total solar irradiance under cloudy regimes were approximately 5 to 10 W m^{-2} greater and 10 to 20 W m^{-2} lower for NOAA 7 and NOAA 11 calibrated data sets, respectively. The NOAA 9 period spanning February 1985 through October 1988 had minimal differences but small feature differences seen reflect the change in treatment of multiple surface reflections (see, for example, Greenland, equation (4)) and the trapping of unexpectedly bad data in the vicinity of topography (section A2) and better data filling schemes (section A3).

Acknowledgments. This research was funded by NASA grant NAGW 2189 to (J.K.B.B.) at Columbia University. The authors would like to thank Bruce W. Forgan (BOM, Australia) for his help with the Cape Grim data set and for detailed comments on the paper; Inez Fung for very helpful discussions; and Jamie McLaren and Zulema Garraffo (Columbia Univeristy) for help with the production of the data sets.

References

Bishop, J.K.B., and W.B. Rossow, Spatial and temporal variability of global surface solar irradiance, *J. Geophys. Res., 96,* 16,839-16,858, 1991.

Bishop, J.K.B., R.C. Smith, and K. Baker, Springtime distributions and variability of biogenic particulate matter in Gulf Stream warm-core ring 82B and surrounding N.W. Atlantic waters, *Deep Sea Res., 1A,* S295-S325, 1992.

Bodhaine, B., E. Dutton, R. Evans, R. Grass, J. Harris, D. Hofmann, W. Komhyr, D. Nelson, J. Ogren, and S. Oltmans, Aerosol, Radiation, ozone, and water vapor division. in *Climate Monitoring and Diagnostics Laboratory Summary Report 1993*, edited by J.T. Petterson and R.M. Rosson, pp. 31-65. U.S. Dep. of Comm., 1993.

Brest, C.L., W.B. Rossow, and M.D. Roiter, Update on ISCCP calibrations for visible and infrared radiances, *J. Atmos. Oceanic Technol.*, in press, 1997.

Cess, R.D., *et al.,* Absorption of solar radiation by clouds: Observations versus models, *Science, 267,* 496-499, 1995.

Chadwick, M.J., and J.C. Kuylenstirena, The relative sensitivity of ecosystems in Europe to acidic depositions. A preliminary assessment of the sensitivity of aquatic and terrestrial ecosystems, Stolkholm Environment Institute Sweden, *in Acidic Deposition, Its Nature and Impacts*, edited by F.T. Last and R. Watling, R. Soc. of Edinburgh, 1991.

Darnell, W.L., W.F. Staylor, S.K. Gupta, and F.M. Dunn, Estimations of surface solar insolation using sun-synchronous satellite data, *J. Clim., 1,* 820–835, 1988.

Deser, C., and M.L. Blackman, Surface climate variations over the North Atlantic Ocean during winter: 1900-1989, *J. Clim., 6,* 1743-1753. 1993.

Dickey, T., *et al.,* Seasonal variability of biooptical properties in the Sargasso Sea, *J. Geophys. Res., 98,* 865-898, 1993.

Dickey, T.D. J. Marra, M. Stramska, C. Langdon, T. Granata, R. Weller, A. Plueddueann, and J. Yoder, Biooptical and physical variability in the subarctic North Atlantic Ocean during the spring of 1989, *J. Geophys. Res., 99,* 22,541-22,556, 1994.

Dobson, F.W., and S.D. Smith, Bulk models of solar radiation at sea, *Q. J. R. Meteorol. Soc , 114,* 165–182, 1988.

Frouin, R., and J. J. Simpson, Radiometric calibration of VISSR solar channels during the GOES pathfinder benchmark period, *Remote Sens. Environ., 52,* 95-115. 1995.

Frouin, R., D.W. Lingner, C. Gautier, K.S. Baker, and R.C. Smith, A simple analytical formula to compute clear sky total and photosynthetically available solar irradiance at the ocean surface, *J. Geophys. Res., 94,* 9731-9742, 1989.

Gautier, C., G.R. Diak, and S. Masse, A simple physical model to estimate incident solar radiation at the sea surface from GOES satellite data, *J. Appl. Meteorol., 19,* 1005–1012, 1980.

Hayes, S.P., L.J. Mangum, J. Picaut, A. Sumi, and K. Takeuchi, TOGA-TAO: A moored array for realtime measurements in the tropical Pacific Ocean, *Bull. Am. Meteorol. Soc., 72,* 339-347, 1991.

Hooker, S.B. and W.E. Esaias, An overview of the SeaWiFS project, *Eos Trans. AGU, 74,* 245-246, 1993.

Kahru, M., U. Horstmann, and O. Rud, Satellite detection of increased cyanobacteria blooms in the Baltic Sea: Natural fluctuation or ecosystem change?, *Ambio, 23,* 469-472, 1994.

Klein, S.A., and D.L. Hartmann, Spurious changes in the ISCCP dataset, *Geophys. Res. Lett., 20,* 455-458, 1993.

Langner, J. and H. Rodhe, A global three-dimensional model of the tropospheric sulfur cycle, *J Atmos. Chem., 13,* 255-263, 1991.

Levitus, S., J. I. Antonov, and T.P. Boyer, Interannual variability of temperature at a depth of 125 meters in the North Atlantic Ocean, *Science, 266,* 96-99, 1994.

Li, Z. Intercomparison between two satellite-based products of net surface shortwave radiation, *J. Geophys. Res., 100,* 3221-3232, 1995.

Li, Z., and H.G. Leighton, Global climatology of solar radiation budgets at the surface and in the atmosphere from 5 years of ERBE data, *J. Geophys. Res., 98,* 4919-4930, 1993.

Liu, W.T., A. Zhang, and J.K.B. Bishop, Evaporation and solar irradiance as regulators of sea surface temperature in annual and interannual changes, *J. Geophys. Res., 99,* 12,623-12,637, 1994.

MacWhorter, M.A., and R.A. Weller, Error in measurements of incoming shortwave radiation made from ships and buoys, *J. Atmos. Ocean. Technol. 8,* 108-117, 1991.

Mitchell, B.G., E. Brody, O. Holm-Hansen, C. McClain, and J.K.B. Bishop, Light limitation of phytoplankton biomass and macronutrient utilization in the Southern Ocean, *Limnol. Oceanogr., 36,* 1662-1677. 1991.

Ohmura, A., and H. Gligen, Global Energy Balance Archive (GEBA), *World Clim. Program - Water Proj. A7, Rep. 2,* 60 pp., GEBA Database, Interactive Appl. Retrieving Data, Ver. der Fachverelne, Zurich, 1991.

Oort, A. H., *Global Atmospheric Circulation Statistics,* 1958-1973. NOAA Prof. Pap. 14, 180 pp, 47 microfiches, U.S. Gov. Print. Off., Washington, D.C., 1983.

Pinker, R.T., I. Laszlo, C.H. Whitlock, and T.P. Charlock, Radiative flux opens new window on climate research, *Eos Trans. AGU,* 76 (15), 145, 155, 158, 1995.

Plueddeman, A.J., R.A. Weller, M. Stramska, T.D. Dickey, and J.Marra, The vertical structure of the upper ocean during the Marine Light - Mixed Layers Experiment, *J. Geophys. Res., 100,* 6606-6620, 1995.

Potter, C.S., J.T. Randerson, C.B. Field, P.A. Matson, P.M. Vitousek, H.A. Mooney, and S. A. Klooster, Terrestrial ecosystem production: A process model based on global satellite and surface data, *Global Biogeochem. Cycles, 7,* 811-841, 1993.

Rossow, W.B., and B. Cairns, Monitoring changes of clouds, *Clim. Change, 31,* 305-347. 1995.

Rossow, W.B., and R.A. Schiffer, ISCCP cloud data products, *Bull. Am. Meteorol. Soc., 72,* 2-20, 1991.

Rossow, W.B., et al., ISCCP cloud algorithm intercomparison, *J. Clim. Appl. Meteorol., 24,* 877-903, 1985.

Rossow, W.B., L.C. Garder, P-J. Lu, and A.W. Walker, International Satellite Cloud Climatology Project (ISCCP) documentation of cloud data. *WMO/TD-266,* 78 pp, 2 appendices, World Meteorol. Organ., Geneva, 1988.

Rossow, W.B., and Y.-C. Zhang, Calculation of surface and top-of-atmosphere radiative fluxes from physical quantities based on ISCCP data sets, II, Validation and first results, *J. Geophys. Res., 100,* 1167-1197, 1995.

Schiffer, R.A., and W.B. Rossow, The international satellite cloud climatology project (ISCCP): The first project of the World Climate Research Program, *Bull. Am Meteorol. Soc., 64,* 779-784, 1983.

Schiffer, R.A., and W.B. Rossow, ISCCP global radiance data set: A new resource for climate research, *Bull. Am. Meteorol. Soc., 66,* 1498-1505, 1985.

Seager, R., and M. B. Blumenthal, Modeling tropical Pacific sea surface temperature with satellite-derived solar radiative forcing, *J. Clim., 7,* 1943-1957, 1994.

Seze, G., and W.B. Rossow, Effects of satellite data resolution on space/time variations of surfaces and clouds, *Int. J. Remote Sensing, 12,* 921-952, 1991.

Smith, S.D., and F.W. Dobson, The heat budget at ocean weather station Bravo, *Atmos. Ocean, 22,* 1–22, 1984.

Stowe, L.L., R.M. Carey, and P.P. Pellegrino, Monitoring the Mt. Pinatubo

aerosol layer with NOAA/AVHRR data, *Geophys. Res. Lett., 19,* 159-162, 1992.

Stramska, M., T.D. Dickey, A. Plueddemann, R. Weller, C. Langdon, and J. Marra. Biooptical variability associated with phytoplankton dynamics in the North Atlantic Ocean during the spring and summer of 1991, *J Geophys Res , 100,* 6621-6632, 1995.

Tarpley, J.D., Estimating incident solar radiation at the surface from geostationary satellite data, *J. Appl. Meteorol., 18,* 1172–1181, 1979.

Tegen, I., and I. Fung, Modelling of mineral dust in the atmosphere: Sources, transport, and optical thickness, *J. Geophys. Res., 99,* 22,827-22,914, 1994.

Tegen, I., and I. Fung, Contribution to the atmospheric mineral aerosol load from land surface modification, *J. Geophys. Res., 100,* 18,707-18,726, 1995.

Whitlock, C.H., et al., Comparison of surface radiation budget satellite algorithms for downwelled shortwave irradiance with Wisconsin FIRE/SRB surface-truth data, paper presented at the Seventh Conference on Atmospheric Radiation, Am. Meteorol. Soc., San Francisco, July 23–27, 1990.

World Climate Research Program (WCRP), radiation and climate, in *Second Workshop on the Implementation of the Baseline Surface Radiation Network, WCRP-64, WMO/TD-453,* Geneva, 1991.

Zhang, Y-C., W.B. Rossow, and A.A. Lacis, Calculation of surface and top-of-atmosphere radiative fluxes from physical quantities based on ISCCP data sets, 1, Method and sensitivity to input data uncertainties, *J. Geophys Res , 100,* 1149-1165, 1995.

Zuill, W., *Bermuda Journey: A Leasurely Guidebook,* 426 pp., Robert MacLehose Univ Press, Glasgow, 1946.

J. K. B. Bishop, School of Earth and Ocean Sciences, University of Victoria, P. O. Box 3055, Victoria, BC, Canada V8W 3P6. (e-mail: bishop@flamingglo.seos.uvic.ca)

E. G. Dutton, NOAA, Climate Monitoring and Diagnostics Laboratory, 325 Broadway, Boulder, CO, USA, 80303-3328. (e-mail: dutton@cmdl1.cmdl.noaa.gov)

W. B. Rossow, NASA Goddard Institute for Space Studies, Goddard Space Flight Center, 2880 W Broadway, New York, NY 10025. (e-mail: clwbr@nasagiss.giss.nasa.gov)

(Received February 29, 1996; revised December 3, 1996; accepted December 3, 1996.)